Han, H., Tanigaki, K., Yamamoto, N., Kuroda, K., Yoshimoto, M., Nakahata, T., Ikuta, K., and Honjo, T. (2002). Inducible gene knockout of transcription factor recombination signal binding protein-J reveals its essential role in T versus B lineage decision. Int. Immunol. *14*, 637–645.

Heller, R.S., Jenny, M., Collombat, P., Mansouri, A., Tomasetto, C., Madsen, O.D., Mellitzer, G., Gradwohl, G., and Serup, P. (2005). Genetic determinants of pancreatic epsilon-cell development. Dev. Biol. *286*, 217–224.

Hrabé de Angelis, M., McIntyre, J., II, and Gossler, A. (1997). Maintenance of somite borders in mice requires the Delta homologue Dll1. Nature *386*, 717–721.

Ishibashi, M., Ang, S.L., Shiota, K., Nakanishi, S., Kageyama, R., and Guillemot, F. (1995). Targeted disruption of mammalian hairy and Enhancer of split homolog-1 (HES-1) leads to up-regulation of neural helix-loop-helix factors, premature neurogenesis, and severe neural tube defects. Genes Dev. *9*, 3136–3148.

Jensen, J., Pedersen, E.E., Galante, P., Hald, J., Heller, R.S., Ishibashi, M., Kageyama, R., Guillemot, F., Serup, P., and Madsen, O.D. (2000a). Control of endodermal endocrine development by Hes-1. Nat. Genet. *24*, 36–44.

Jensen, J., Heller, R.S., Funder-Nielsen, T., Pedersen, E.E., Lindsell, C., Weinmaster, G., Madsen, O.D., and Serup, P. (2000b). Independent development of pancreatic alpha- and beta-cells from neurogenin3-expressing precursors: a role for the notch pathway in repression of premature differentiation. Diabetes *49*, 163–176.

Kageyama, R., and Ohtsuka, T. (1999). The Notch-Hes pathway in mammalian neural development. Cell Res. *9*, 179–188.

Kato, H., Sakai, T., Tamura, K., Minoguchi, S., Shirayoshi, Y., Hamada, Y., Tsujimoto, Y., and Honjo, T. (1996). Functional conservation of mouse Notch receptor family members. FEBS Lett. *395*, 221–224.

Kojima, M., Hosoda, H., Date, Y., Nakazato, M., Matsuo, H., and Kangawa, K. (1999). Ghrelin is a growth-hormone-releasing acylated peptide from stomach. Nature *402*, 656–660.

Lammert, E., Brown, J., and Melton, D.A. (2000). Notch gene expression during pancreatic organogenesis. Mech. Dev. *94*, 199–203.

Miyamoto, Y., Maitra, A., Ghosh, B., Zechner, U., Argani, P., Iacobuzio-Donahue, C.A., Sriuranpong, V., Iso, T., Meszoely, I.M., Wolfe, M.S., et al. (2003). Notch mediates TGF alpha-induced changes in epithelial differentiation during pancreatic tumorigenesis. Cancer Cell *6*, 565–576.

Murtaugh, L.C., and Melton, D.A. (2003). Genes, signals, and lineages in pancreas development. Annu. Rev. Cell Dev. Biol. *19*, 71–89.

Murtaugh, L.C., Stanger, B.Z., Kwan, K.M., and Melton, D.A. (2003). Notch signaling controls multiple steps of pancreatic differentiation. Proc. Natl. Acad. Sci. USA *100*, 14920–14925.

Oka, C., Nakano, T., Wakeham, A., de la Pompa, J.L., Mori, C., Sakai, T., Okazaki, S., Kawaichi, M., Shiota, K., Mak, T.W., and Honjo, T. (1995). Disruption of the mouse RBP-J kappa gene results in early embryonic death. Development *121*, 3291–3301.

Pang, K., Mukonoweshuro, C., and Wong, G.G. (1994). Beta cells arise from glucose transporter type 2 (Glut2)-expressing epithelial cells of the developing rat pancreas. Proc. Natl. Acad. Sci. USA *91*, 9559–9563.

Pictet, R., and Rutter, W.J. (1972). Development of the embryonic endocrine pancreas. In Handbook of Physiology, Section 7, D.F. Steiner and N. Frenkel, eds. (Baltimore, MD: Williams and Williams), pp. 25–66.

Pui, J.C., Allman, D., Xu, L., DeRocco, S., Karnell, F.G., Bakkour, S., Lee, J.Y., Kadesch, T., Hardy, R.R., Aster, J.C., and Pear, W.S. (1999). Notch1 expression in early lymphopoiesis influences B versus T lineage determination. Immunity *11*, 299–308.

Schwitzgebel, V.M., Scheel, D.W., Conners, J.R., Kalamaras, J., Lee, J.E., Anderson, D.J., Sussel, L., Johnson, J.D., and German, M.S. (2000). Expression of neurogenin3 reveals an islet cell precursor population in the pancreas. Development *127*, 3533–3542.

Swiatek, P.J., Lindsell, C.E., del Amo, F.F., Weinmaster, G., and Gridley, T. (1994). Notch1 is essential for postimplantation development in mice. Genes Dev. *15*, 707–719.

Thorens, B., Wu, Y.J., Leahy, J.L., and Weir, G.C. (1992). The loss of GLUT2 expression by glucose-unresponsive cells of db/db mice Is reversible and is induced by the diabetic environment. J. Clin. Invest. *90*, 77–85.

Tomita, K., Moriyoshi, K., Nakanishi, S., Guillemot, F., and Kageyama, R. (2000). Mammalian achaete-scute and atonal homologs regulate neuronal versus glial fate determination in the central nervous system. EMBO J. *19*, 5460–5472.

Wilson, A., MacDonald, H.R., and Radtke, F. (2001). Notch 1-deficient common lymphoid precursors adopt a B cell fate in the thymus. J. Exp. Med. *194*, 1003–1012.

Xue, Y., Gao, X., Lindsell, C.E., Norton, C.R., Chang, B., Hicks, C., Gendron-Maguire, M., Rand, B., Weinmaster, G., and Gridley, T. (1999). Embryonic lethality and vascular defects in mice lacking the Notch ligand Jagged1. Hum. Mol. Genet. *8*, 723–730.

0013-7227/06/$15.00/0
Printed in U.S.A.

Endocrinology 147(4):1642–1653

doi: 10.1210/en.2005-1038

The Neuroprotective and Vasculo-Neuro-Regenerative Roles of Adrenomedullin in Ischemic Brain and Its Therapeutic Potential

Kazutoshi Miyashita, Hiroshi Itoh, Hiroshi Arai, Takayasu Suganami, Naoki Sawada, Yasutomo Fukunaga, Masakatsu Sone, Kenichi Yamahara, Takami Yurugi-Kobayashi, Kwijun Park, Naofumi Oyamada, Naoya Sawada, Daisuke Taura, Hirokazu Tsujimoto, Ting-Hsing Chao, Naohisa Tamura, Masashi Mukoyama, and Kazuwa Nakao

Department of Medicine and Clinical Science (K.M., H.I., H.A., N.S., Y.F., M.S., K.Y., T.Y.-K., K.P., N.O., N.S., D.T., H.T., N.T., M.M., K.N.), Kyoto University Graduate School of Medicine, Kyoto 606-8507, Japan; Department of Molecular Medicine and Metabolism (T.S.), Medical Research Institute, Tokyo Medical and Dental University, Tokyo 101-0062, Japan; and Department of Medicine (T.-H.C.), National Cheng-Kung University Medical Center, Tainan, Taiwan 701, Republic of China

Adrenomedullin (AM) is a vasodilating hormone secreted mainly from vascular wall, and its expression is markedly enhanced after stroke. We have revealed that AM promotes not only vasodilation but also vascular regeneration. In this study, we focused on the roles of AM in the ischemic brain and examined its therapeutic potential. We developed novel AM-transgenic (AM-Tg) mice that overproduce AM in the liver and performed middle cerebral artery occlusion for 20 min (20m-MCAO) to examine the effects of AM on degenerative or regenerative processes in ischemic brain. The infarct area and gliosis after 20m-MCAO was reduced in AM-Tg mice in association with suppression of leukocyte infiltration, oxidative stress, and apoptosis in the ischemic core. In addition, vascular regeneration and subsequent neurogenesis were enhanced in AM-Tg mice, preceded by increase in mobilization of CD34$^+$ mononuclear cells, which can differentiate into endothelial cells. The vasculo-neuro-regenerative actions observed in AM-Tg mice in combination with neuroprotection resulted in improved recovery of motor function. Brain edema was also significantly reduced in AM-Tg mice via suppression of vascular permeability. *In vitro*, AM exerted direct antiapoptotic and neurogenic actions on neuronal cells. Exogenous administration of AM in mice after 20m-MCAO also reduced the infarct area, and promoted vascular regeneration and functional recovery. In summary, this study suggests the neuroprotective and vasculo-neuro-regenerative roles of AM and provides basis for a new strategy to rescue ischemic brain through its multiple hormonal actions. (*Endocrinology* 147: 1642–1653, 2006)

ADRENOMEDULLIN (AM) IS a potent vasodilating peptide comprising 52 amino acids, which was originally isolated from human pheochromocytoma tissues in 1993 as a substance to elevate cAMP concentration in platelets (1). It is secreted mainly from the vascular wall into circulating blood to reduce pre- and post-load on the heart via vasodilation, natriuresis, and suppression of aldosterone release. Intravenous administration of AM to patients with heart failure or pulmonary hypertension has already been initiated and beneficial hemodynamic effects have been reported (2).

First Published Online December 29, 2005

Abbreviations: AM, Adrenomedullin; ANCOVA, analysis of covariance; BP, blood pressure; BrdU, bromodeoxyuridine; CGRP, calcitonin gene-related peptide; diHE, dihydroethidium; GFAP, glial fibrillary acidic protein; LDPI, laser Doppler perfusion imager; MCA, middle cerebral artery; 20m-MCAO, middle cerebral artery occlusion for 20 min; NeuN, neuronal marker; NHNP, normal human neuronal progenitor cells; PAMP, proadrenomedullin N-terminal 20 peptide; PECAM, platelet endothelial cell adhesion molecule; PI3K, phosphatidyl inositol-3 kinase; PKA, protein kinase A; ROS, reactive oxygen species; ssDNA, single-strand DNA; Tg, transgenic; Wt, wild type.

Endocrinology is published monthly by The Endocrine Society (http://www.endo-society.org), the foremost professional society serving the endocrine community.

Along with its vasodilating effect, a number of studies have demonstrated various and significant effects of AM on the regulation of vascular structure, including its development, remodeling, and regeneration. Mice lacking the AM gene did not survive their embryonic stage and showed abnormal vasculature with sc hemorrhage (3, 4). Mice overexpressing AM in endothelial cells were revealed to be hypotensive and resistant to vascular remodeling such as neointima formation caused by cuff injury, and atherogenesis associated with a high-cholesterol diet (5). We have recently established that AM promotes endothelial regeneration in the wound healing assay using cultured endothelial cells and enhances neovascularization *in vivo* into sc implanted gelplugs in mice (6, 7). We and others (8–11) have further demonstrated that the potentiating action of AM on vascular regeneration is mediated by activation of the phosphatidyl inositol-3 kinase (PI3K)-Akt pathway.

Recently, it has been known that AM is secreted from various organs including the heart, lung, kidney, adipose tissues, and central nervous system (12). Moreover, AM expression has been demonstrated to be markedly enhanced by ischemia through the activation of hypoxia-responsive elements in the AM gene via transcription factor hypoxia-inducible factor-1. In the central nervous system, where AM is

mainly expressed in neurons and the endothelium (13), it is reported that transient ischemia boosted AM expression for more than 15 d (14). However, the role of augmented AM has remained unclear for inconsistent previous results: three studies reported neuroprotective effects of AM by demonstrating reduction of infarct size after transient ischemia (15–17), whereas one study detected exacerbation of infarction as a result of AM infusion (14).

In this context, our study presented here focused on the roles of augmented AM in ischemic brain and examined its therapeutic potential. We generated new lines of transgenic mice that overproduce AM (AM-Tg) in the liver that mimics chronic AM administration. After inducing 20-min middle cerebral artery occlusion (20m-MCAO) to produce a nonfatal stroke model in the AM-Tg mice, we observed the long-term effects of AM on the ischemic brain up to postoperative d 56. We examined the mice for the recovery of blood flow in the ischemic region and impaired motor function after stroke, and immunohistochemically examined the ischemic striatum to determine effects of AM on neuronal loss/apoptosis, gliosis, leukocyte infiltration, oxidative stress, vascular regeneration, and neurogenesis after 20m-MCAO. In addition, another stroke model, 2-h middle cerebral artery occlusion (2 h-MCAO), was performed to observe the effect of AM in acute phase of the fatal stroke. *In vitro* studies using neuronal progenitor cells or rat pheochromocytoma PC12 cells were performed to examine direct antiapoptotic and neurogenic actions of AM on these neuronal cells. Finally, we investigated the effect of exogenous AM administration after 20m-MCAO to determine the appropriate amount and timing of AM treatment after cerebral ischemia.

Materials and Methods

Generation of transgenic mice which overproduce human AM but do not overproduce mature proadrenomedullin N-terminal 20 peptide (PAMP)

The AM gene contains coding regions for not only AM but also PAMP, a different vasodilating peptide. Amidation at their carboxyl terminals after their synthesis is needed for both AM and PAMP to exert their biological activity. The bioactive amidated forms are known as mature AM and mature PAMP, respectively. To identify the specific effects of AM, we generated a transgene construct with a point mutation on the PAMP amidation signal in the full-length AM gene cDNA. Guanine was substituted for cytosine on the 3′ end of the PAMP coding region so that glycine on the C′ terminal of the PAMP product was replaced with alanine. In this way, amidation and maturation of PAMP by peptidylglycine α-hydroxylase and α-hydroxyglycine N-C lyase were inhibited (Fig. 1A). The mutant AM gene cDNA was then inserted into a plasmid containing the human serum amyloid P component promoter, which is widely used to target gene expression specific to the liver. When the product is secreted from the liver, it mimics intravenous administration of the agent. The *Hin*dIII-*Xho*I fragment of the plasmid was microinjected into the pronucleus of fertilized C57BL/6J mice eggs.

The copy number of transgenes was quantified by means of genomic Southern blotting according to standard procedure. Plasma concentrations of human total AM and mature AM were measured with a commercially available immunoradiometric assay (Cosmic, Tokyo, Japan).

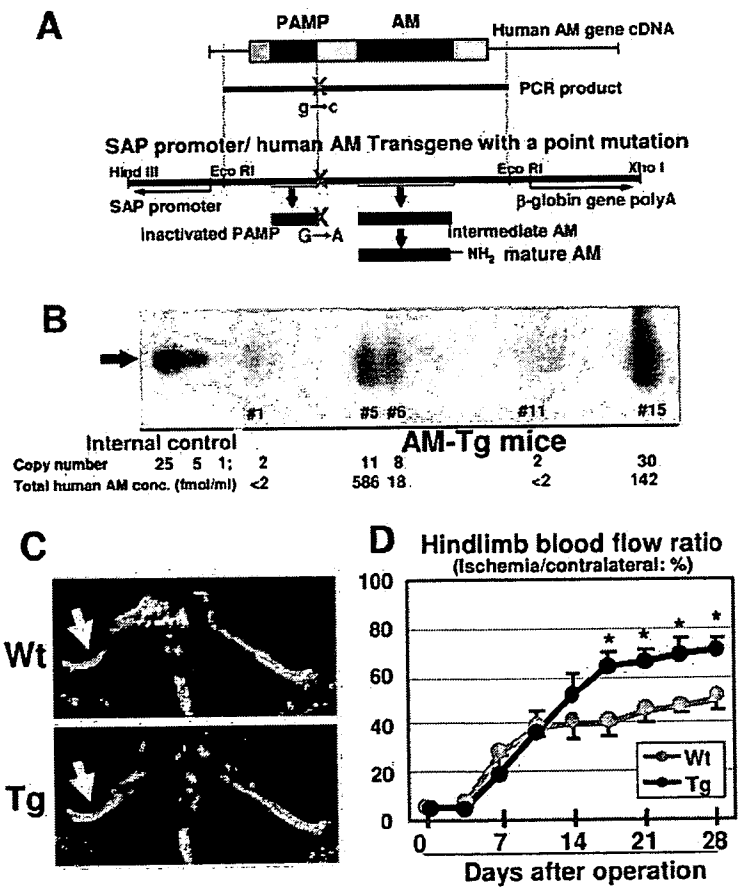

FIG. 1. Generation of transgenic mice which overproduce AM but do not overproduce mature PAMP in the liver and augmented angiogenesis in the transgenic mice after femoral artery occlusion. A, Schematic representation of the transgene construct derived from human AM gene cDNA with a point mutation in the amidation signal of PAMP. B, Southern blot analysis of the tail DNA of the founder mice. *Arrow*, Blots for the transgene. Internal controls for indicated copies are located in the *left three lanes*. The line No. indicates the mice in which the transgene was detected by PCR. The copy numbers estimated by densitometry and the plasma concentrations of total human AM in F3 mice of the lines are shown. C, Hindlimb blood flow analyzed by LDPI. *Red* or *white* indicates a higher flow than *blue* or *green*. *Arrows*, Comparison of ischemic hindlimbs between Wt and AM-Tg on d 28 after femoral artery ligation. D, Quantitative analysis of the hindlimb blood flow in ischemia. *, $P < 0.05$ for Wt *vs.* AM-Tg by ANCOVA; n = 6.

Human mature PAMP concentration was measured with a recently developed enzyme immunoassay (18). To determine the brain concentration of AM, we used the RIA kits for measurement of human and mouse total AM (Phoenix, Belmont, CA), according to the manufacturer's instruction. Blood pressure (BP) was measured with tail cuff (Softron, Tokyo, Japan). Hindlimb ischemia was induced by ligating the right femoral artery and blood flow of the ischemic limb was estimated with a laser Doppler perfusion imager (LDPI; Moor Instruments Ltd., Devon, UK) to confirm the angiogenic effect of AM-Tg mice. The perfusion ratio (%) was calculated as that of the ipsilatereal to the contralateral side. Animal care and experiments were in accordance with the guidelines for animal experiments of Kyoto University.

Induction of stroke by MCAO

We performed nonfatal 20m-MCAO and fatal 2 h-MCAO by the standard *trans*-luminal method, which has been described in various previous reports (19). Briefly, a 8–0 nylon monofilament coated with silicone was inserted from the left common carotid artery via the internal carotid to the base of the left middle cerebral artery (MCA) of 12-wk-old mice anesthetized with 5% halothane and maintained on 1%. After 20 min or 2 h of occlusion, the filament was withdrawn; and the arteries were reperfused, whereas the left common carotid artery was permanently ligated. Occlusion and reperfusion of the MCA was confirmed by means of fiber-shaped laser Doppler perfusion imager (Omegawave, Tokyo, Japan). We observed the mice until postoperative d 56 to examine blood flow in the ischemic region with an LDPI and motor function with a rota-rod exercise test.

Immunohistochemical examination of the ischemic striatum

After the induction of 20m-MCAO, mice were killed on postoperative d 0–56 and the harvested brains were subjected to immunohistochemical examination using a standard procedure described elsewhere (20). We used these primary antibodies: neuronal marker, NeuN (1:200; Chemi-Con, Temecula, CA); astrocyte marker, glial fibrillary acidic protein (GFAP) (1:400; Chemicon); apoptosis marker, single-strand DNA (ssDNA) (1:50; Dako, Carpinteria, CA); leukocyte marker, CD45 (1:100, PharMingen, San Diego, CA); endothelial marker, platelet endothelial cell adhesion molecule (PECAM)-1 (CD31) (1:100, PharMingen); and a marker for proliferating cells, bromodeoxyuridine (BrdU) (1:50, Molecular Probes, Eugene, OR); to examine infarct area, gliosis, leukocyte infiltration, apoptosis, vascular regeneration and neurogenesis. Briefly, free-floating 30-μm coronal sections at the level of the anterior commissure were stained and observed with a confocal microscope (LSM5 PASCAL; Carl Zeiss SMT AG, Oberkochen, Germany). The infarct area (mm^2/field) was defined and quantified as the region where loss of NeuN immunoreactivity was observed and gliosis (mm^2/field) as the area stained GFAP in the ischemic striatum at × 5 fields. CD45 or ssDNA-positive cells (cells/mm^2) were quantified to serve as an index of leukocyte infiltration or of apoptosis, respectively, in the ischemic core at ×20 magnification. Capillary density was quantified as the number of PECAM-1-positive cells (cells/mm^2). The vessel counts were performed in the region of ischemic core at 0.5~1.0 mm anterior from the bregma. We prepared two thin sections (6 μm thickness) per mouse for vessel counting and four representative fields from each section were evaluated for capillary density in the ischemic core. To examine neurogenesis, mice were injected ip with BrdU 50 mg/kg (Sigma-Aldrich Co., St. Louis, MO) twice daily on postoperative d 4–6 and the number of BrdU-NeuN double-positive cells (cells/mm^2), which are generally defined as regenerated neurons, were quantified to serve as an index of neurogenesis. We also examined the production of reactive oxygen species (ROS) *in situ* by using the oxidative fluorescent dye dihydroethidium (diHE; 2×10^{-6} M; Sigma).

Quantification of CD34$^+$ mononuclear cells after 20m-MCAO

We counted peripheral $CD34^+$ mononuclear cells according to the International Society of Hematotherapy and Graft Engineering (ISHAGE) guidelines (21). Briefly, peripheral blood was taken from the orbital vein and stained with CD34-PE and CD45-FITC monoclonal antibodies (BD PharMingen, San Jose, CA) in a TruCOUNT tube (BD PharMingen) according to the manufacturer's instruction. After the reaction, $CD34^+$-$CD45^{dim}$ cells were quantified as $CD34^+$ mononuclear cells by a fluorescence-activated cell sorting machine Aria (BD) by using the ISHAGE sequential gating strategy (21).

Analysis of infarct volume and brain edema after 2 h-MCAO

We performed 2 h-MCAO to examine the effect of AM in the acute phase of fatal stroke. To estimate infarct or edema volume, mice were killed 24 h after the occlusion. The brain was removed and cut into 2 mm-thick slices and immersed in saline containing 2% 2,3,5-triphenyltetrazolium chloride for 30 min at 4 C. Infarct or edema volume was calculated as the percentage volume of the contralateral hemisphere with a standard procedure as described elsewhere (22). We estimated Evans Blue leakage in the brain parenchyma as previously reported (23), to serve as an index of vascular permeability *in situ*. Briefly, 0.2 ml of 2.5% Evans Blue solution was injected into mice via a tail vein 10 min before 2 h-MCAO and mice were killed at 24 h after the ischemia. Brain tissues were weighed and homogenized in 50% trichloroacetic acid solution to extract the dye in the supernatant. The tissue content of Evans Blue was estimated from the absorbance of 620 nM.

Estimation of apoptosis and differentiation of neuronal cells

The ratio of apoptotic cells was examined using normal human neuronal progenitor cells (NHNP; Cambrex Bioscience, Walkersville, MD). Cells were plated at a density of 5×10^4 cells/cm^2 on a laminin-coated 24-well dish and incubated in serum-free neuronal basal medium for 48 h. After the experimental period, the cell number was assessed by 5-mercapto-1-methyltetrazole assay (Nakalai Tesque), and the cells were stained with an anti-ssDNA antibody and nuclear staining propidium iodide to calculate the ratio of apoptotic cells to the total cells in each microscopic image.

Neuronal differentiation was examined as described previously (24), using rat pheochromocytoma PC12 cells (Riken Gene Bank, Tsukuba, Japan). Briefly, the length of the neuronal process (micrometers/cell) was calculated to serve as an index of neuronal differentiation after plating at a density of 10^4 cells/cm^2 on a collagen I-coated 24-well dish and incubated in 1% serum DMEM for 7 d. The cells were treated with 10^{-5}mol/liter AM or 100 ng/ml nerve growth factor as a positive control, and with the following inhibitors: the two AM antagonists, 10^{-5}mol/liter AM (22–52) and 10^{-5} mol/liter calcitonin gene-related peptide(8–37) [CGRP(8–37)] (Peptide Institute Inc., Osaka, Japan), the two protein kinase A (PKA) inhibitors, 10^{-5} mol/liter adenosine 3P,5P-cyclic monophosphorothioate Rp-isomer (Rp-cAMP) and 10^{-6} mol/liter myristoylated cell-permeable PKA inhibitor peptide sequence (14–22) (PKA Inh), and the two PI3K inhibitors, 10^{-5} mol/liter LY294002 and 10^{-7} mol/liter wortmannin (Calbiochem, San Diego, CA). For endothelial cell coculture experiments, human umbilical vein endothelial cells (HUVEC; Cambrex) were plated into transwell membrane inserts at a density of 10^5 cells/cm^2.

Exogenous administration of AM and hydralazine

Recombinant human mature AM dissolved in 0.9% saline was exogenously administrated to C57BL/6J wild-type mice (Wt) by means of osmotic pumps (Alzet Model 2002; Alzet Osmotic Pumps Co., Cupertino, CA) at a rate of 50 ng/h, which is estimated to achieve a plasma concentration of 2 fmol/ml (25). To determine appropriate timing to start AM treatment after 20m-MCAO, we implanted the pump ip just after the operation (d 0), or at 24 (d 1) or 72 h (d 3) later. We killed the mice on d 7 for histological examination and the period of the exogenous AM treatment was from d 0, 1, or 3 to d 7. In some experiments, low-dose (0.1 mM) hydralazine was exogenously administrated in drinking water.

Statistics

All data were expressed as mean ± SE. Comparison of means between two groups was performed with Student's *t* test. When more than two groups were compared, ANOVA was used to evaluate significant differences among groups, and if significant differences were confirmed, each difference was further examined by means of multiple comparisons. We

TABLE 1. Plasma concentrations of human AM and systolic BP in Wt and three lines of AM-Tg mice

	Wt	Low conc.	Medium conc.	High conc.
Total AM (fmol/ml)	1.1 ± 0.2	17.6 ± 4.4[a]	142.2 ± 18.4[a]	585.5 ± 117.7[a]
Mature AM (fmol/ml)	0.5 ± 0.4	2.6 ± 0.6[a]	10.4 ± 2.4[a]	24.9 ± 4.2[a]
Systolic BP (mm Hg)	122.7 ± 1.6	113.0 ± 2.5[a]	113.4 ± 2.6[a]	109.4 ± 2.5[a]

conc., Concentration.
[a] $P < 0.01$ *vs.* Wt; n = 4–12.

performed analysis of covariance (ANCOVA) when repeated-measurement had done, specifically, in the rota-rod test and laser Doppler flowmetry. Probability was considered to be statistically significant at $P < 0.05$.

Results

Generation of transgenic mice that overproduce human AM but do not overproduce mature PAMP

We generated seven lines of founder mice carrying the transgene and maintained three of them (lines 5, 6, and 15). Their plasma concentrations of human total AM were 585.5 ± 117.7, 17.6 ± 4.4 and 142.2 ± 18.4 fmol/ml and the copy numbers of the transgene estimated by Southern blot densitometry analysis were 11, 8, and 30, respectively (Fig. 1B). The physiological concentration of mouse total AM is reportedly 5~10 fmol/ml, so that the transgenic mice were expected to overproduce AM about 100, 3, and 30 times more than endogenous AM. The three lines were designated low (no. 6), medium (no. 15), and high (no. 5) concentration line according to their plasma AM concentration. The high concentration line (no. 5) was used for further study unless otherwise indicated. The plasma concentration of human mature AM, the bioactive amidated form, increased to 2.6~24.9 fmol/ml in the AM-Tg mice (Table 1). On the other hand, plasma human mature PAMP did not change in AM-Tg mice. The concentration (fmol/ml) was 2.21 ± 0.58 in Wt *vs.* 2.15 ± 0.35 in AM-Tg (n = 6), so that the point mutation on the amidation signal in the PAMP coding region was expected to successfully inhibit maturation of PAMP. There were no apparent differences in overall appearance, behavior, growth or fertility between Wt and AM-Tg mice. The systolic BP in 12-wk-old mice was significantly reduced in all three lines of AM-Tg compared with Wt. The BP (mm Hg) was 122.7 ± 1.6 in Wt *vs.* 109.4 ± 2.5~113.4 ± 2.6 in AM-Tg, depending on the line ($P < 0.05$; n = 5; Table 1).

Therapeutic angiogenesis in hindlimb ischemia model was promoted in AM-Tg mice

The recovery of blood flow in the ischemic hindlimb of Wt and AM-Tg mice was compared and was found to have

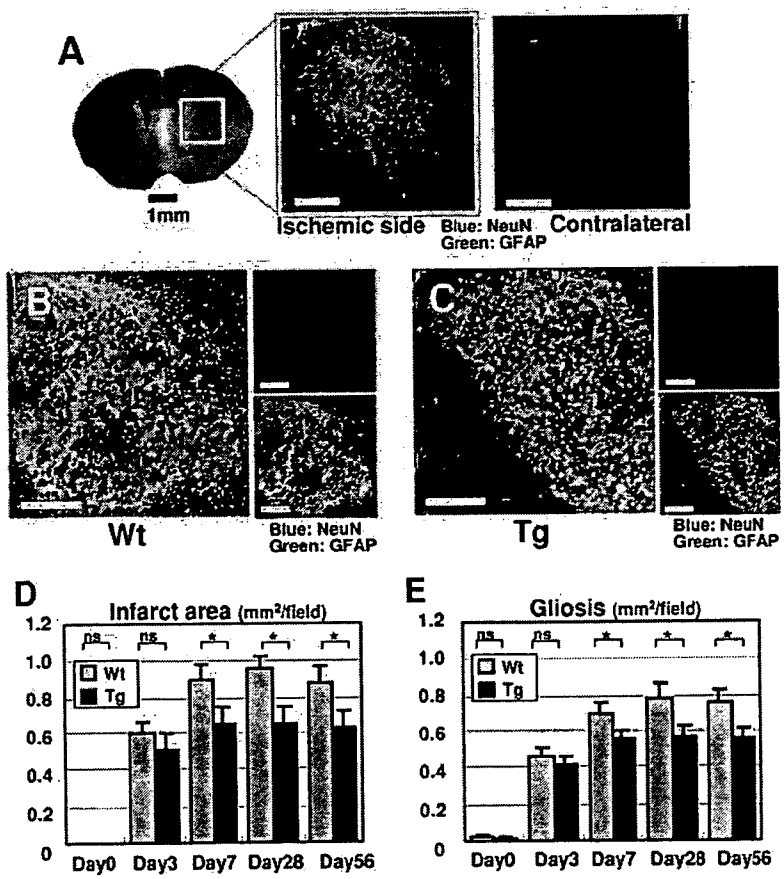

FIG. 2. Effects of AM on infarct area and gliosis after the nonfatal stroke, 20m-MCAO. A, Histological examination of the ischemic striatum. The outlined field was examined for infarct area and gliosis. The ischemic side and contralateral side on d 3 after 20m-MCAO are shown. *Scale bar*, 500 μm (×5 magnification). B and C, Representative images of the ischemic striatum on postoperative d 7 stained for NeuN (*blue*) and GFAP (*green*). Infarct area, defined as the region where NeuN immunoreactivity was lost, and gliosis, defined as the area where GFAP immunoreactivity was observed, in Wt (B) and AM-Tg (C) are shown. *Scale bar*, 500 μm (×5 magnification) D and E, Quantitative analysis of the infarct area (D) and gliosis (E) *, $P < 0.05$; ns, not significant for Wt *vs.* AM-Tg; n = 12.

significantly improved in AM-Tg mice after postoperative d 17. The hindlimb blood flow ratio on d 28 (ipsilateral/contralateral, %) was 56.6 ± 8.3 in Wt *vs.* 73.8 ± 5.3 in AM-Tg ($P < 0.05$; n = 6; Fig. 1, C and D). In this way, promotion of therapeutic angiogenesis by AM was confirmed in AM-Tg mice.

Brain remodeling in ischemic striatum after 20m-MCAO

We investigated the time course of neuronal loss, reactive gliosis, vascular regeneration, and neuronal regeneration; the entire process can be defined as "brain remodeling" after ischemia.

20m-MCAO caused selective loss of NeuN-positive cells and marked reactive gliosis (Fig. 2A) in the ipsilateral striatum within 24 h after the operation; this condition was different from pan-necrosis caused by longer MCAO (*e.g.* 2 h-MCAO). The infarct area, that is, the area of neuronal loss, expanded progressively up to d 7, and then showed gradual increase in size until d 56, whereas gliosis spread in parallel. The expansion of the infarct area in the subacute to chronic phase after mild stroke was compatible with previously reported findings (26). Vascular regeneration in the striatum with enhanced capillary density was obvious after postoperative d 7, and subsequent neurogenesis became obvious after d 28.

The concentrations of the overproduced human AM (fmol/g tissue) in the ischemic brain of AM-Tg mice before and on postoperative d 1 and 28 after 20m-MCAO were 27.8 ± 10.3, 87.4 ± 4.0 and 30.3 ± 16.8, respectively. Those of endogenous mouse AM (fmol/g tissue) were 3.7 ± 2.1, 7.2 ± 2.5, and 4.6 ± 3.0.

Infarct area and gliosis were reduced in AM-Tg mice after 20m-MCAO along with suppression of leukocyte infiltration and ROS production

A significant decrease in infarct area and gliosis was observed in AM-Tg mice (Fig. 2, B–E) after postoperative d 7, but was not obvious on d 3. The infarct area (mm^2/field) on d 56 was 0.88 ± 0.08 in Wt *vs.* 0.64 ± 0.08 in AM-Tg ($P < 0.05$; n = 12; Fig. 2D), and gliosis (mm^2/field) on the same day was 0.76 ± 0.08 in Wt and 0.56 ± 0.07 in AM-Tg ($P < 0.05$; n = 12; Fig. 2E). Leukocyte infiltration quantified as the number of $CD45^+$ cells was significantly suppressed in AM-Tg mice especially from d 3–7. $CD45^+$ cells on d 3 ($/mm^2$) numbered 197.5 ± 16.6 in Wt *vs.* 140.7 ± 14.6 in AM-Tg ($P < 0.05$; n = 12; Fig. 3, A, B, and G). *In situ* ROS production detected by immunostaining for diHE, which stained the nucleus of $NeuN^+$ or $GFAP^+$ cells, was enhanced in Wt compared with that in AM-Tg mice (Fig. 3, C and D). Apoptotic cells quantified as the number of $ssDNA^+$ cells in the ischemic core were significantly reduced in the AM-Tg mice on d 3–7. $ssDNA^+$ cells ($/mm^2$) on d 3 numbered 214.8 ± 19.6 in Wt *vs.* 123.2 ± 11.1 in AM-Tg ($P < 0.01$; n = 12; Fig. 3, E, F, and H).

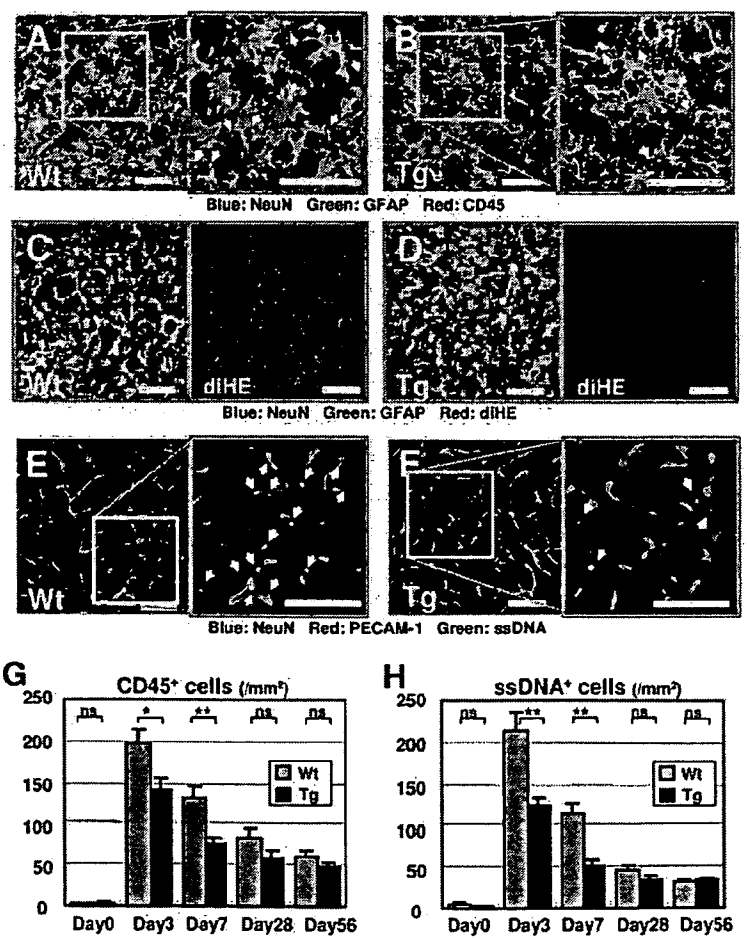

FIG. 3. Effects of AM on leukocyte infiltration, ROS production, and apoptosis in the ischemic brain after 20m-MCAO. A and B, Detection of leukocyte infiltration in the ischemic core on postoperative d 7 by immunostaining for $CD45^+$ cells (*red*) in Wt (A) and AM-Tg (B). *Arrows*, $CD45^+$ cells. C and D, *In situ* detection of ROS in ischemic striatum on postoperative d 7 by immunostaining for diHE (*red*) in Wt (C) and AM-Tg (D). E and F, Detection of apoptotic cells in the ischemic core on postoperative d 7 by immunostaining for $ssDNA^+$ cells (*green*) in Wt (E) and AM-Tg (F). *Arrows*, $ssDNA^+$ cells. G and H, Quantitative analysis of $CD45^+$ cells (G) and $ssDNA^+$ cells (H) in the ischemic core. *, $P < 0.05$; **, $P < 0.01$; ns, not significant for Wt *vs.* AM-Tg; n = 12. *Scale bar*, 100 μm (×20 magnification).

Vascular regeneration was augmented in AM-Tg mice after 20m-MCAO associated with increased mobilization of CD34$^+$ mononuclear cells

The blood flow in the ischemic brain estimated by LDPI was significantly higher in AM-Tg mice after postoperative d 7 and higher flow was maintained until d 56. The brain blood flow ratio (ipsilateral/contralateral, %) on d 56 was 88.9 ± 2.8 in Wt *vs.* 97.6 ± 3.0 in AM-Tg ($P < 0.01$ by ANCOVA; n = 8; Fig. 4, C, D, and H). We were also able to confirm that capillary density determined as the number of PECAM-1$^+$ cells was augmented in AM-Tg mice. The density (/mm^2) on d 56 was 468.8 ± 21.8 in Wt *vs.* 536.6 ± 13.6 in AM-Tg ($P < 0.05$; n = 8; Fig. 4I). Thus, the physiological neovascularization in the ischemic core after stroke was augmented in AM-Tg mice. Peripheral CD34$^+$ mononuclear cells were physiologically enhanced after 20m-MCAO and further increased in AM-Tg mice on d 3–7. The cells (/ml) on d 3 numbered 1774 ± 272 in Wt *vs.* 3199 ± 562 in AM-Tg ($P < 0.05$; n = 6; Fig. 5, A–C).

Augmented neurogenesis and improved recovery of impaired neurological function were observed in AM-Tg mice after 20m-MCAO

BrdU injection on postoperative d 4~6 proved that most BrdU-positive cells were costained with GFAP (data not shown) and that there were far fewer BrdU-PECAM-1 or BrdU-NeuN double-positive cells. We found that regenerated neurons defined as BrdU-NeuN double-positive cells were frequently detected adjacent to the vasculature and the number of these cells on d 56 was correlated with capillary density ($P = 0.003$; n = 12; Fig. 6, A and B; and Table 2). The cells increased from postoperative d 7–56, and their number was significantly higher in AM-Tg mice. The regenerated neurons (/mm^2) on d 56 numbered 20.4 ± 3.9 in Wt *vs.* 33.9 ± 4.7 in AM-Tg ($P < 0.05$; n = 12; Fig. 6C).

Recovery of impaired motor function after 20m-MCAO, quantified as the exercise time on an accelerating rota-rod from the start to collapse down, was significantly better in AM-Tg mice. The exercise time (second) on d 49 was 21.5 ± 1.5 for Wt *vs.* 27.1 ± 2.0 for AM-Tg ($P < 0.01$ by ANCOVA; n = 14; Fig. 6D). To confirm whether vasculogenesis and neurogenesis are the contributing factor to the recovery from the ischemic damage, we analyzed the relation between capillary density, the number of regenerated neuron and the rota-rod result in AM-Tg mice after 20m-MCAO. As shown in Table 2, we found that the capillary density was significantly correlated with the rota-rod exercise time ($P = 0.005$; n = 24) and neurogenesis tended to be correlated with it ($P = 0.08$; n = 12).

Low-concentration AM-Tg mice also showed reduced infarct area and promoted vascular regeneration

We performed 20m-MCAO, using the low-concentration AM-Tg mice (plasma mature AM, 2.6 ± 0.6 fmol/ml) as well as the high-concentration line (plasma mature AM, 24.9 ± 4.2 fmol/ml) to determine appropriate concentration for AM

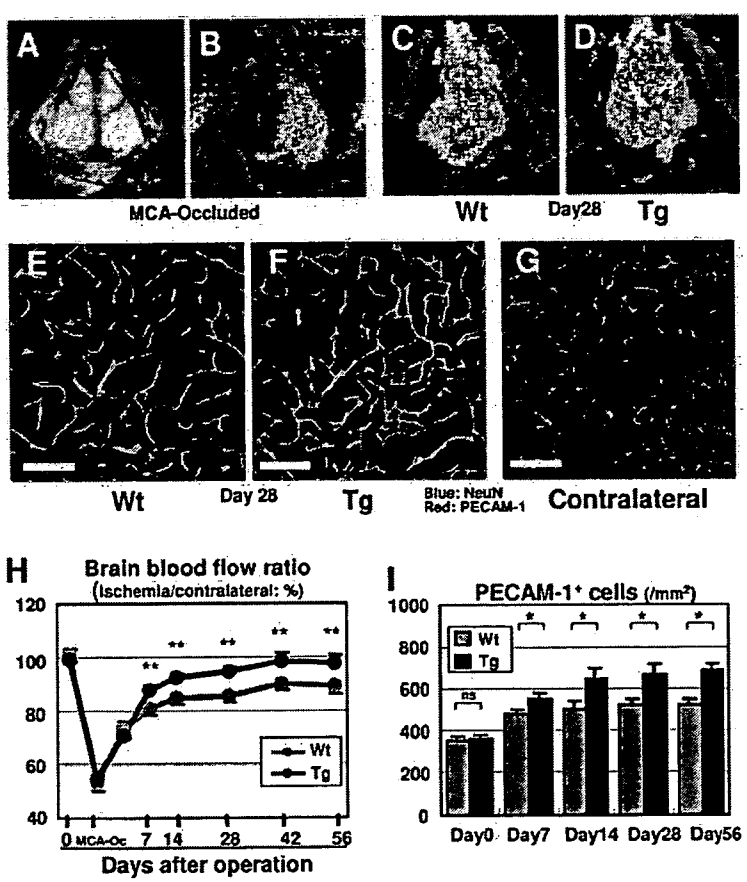

FIG. 4. Effects of AM on vascular regeneration in the ischemic brain after 20m-MCAO. A–D, Analysis of the blood flow in the ischemic brain by LDPI evaluated in mice with the scalp removed (A). Flowmetric analysis of the ischemic brain during MCA-Occlusion (B) and on d 28 after 20m-MCAO in Wt (C) and AM-Tg (D). *Red* or *white* indicates higher flow than *blue* or *green*. E–G, Histological examination of the vasculature in the ischemic core with PECAM-1 staining. Ischemic striatum on d 28 after 20m-MCAO in Wt (E) and AM-Tg (F), and contralateral nonischemic striatum (G). *Scale bar*, 100 μm (×20 magnification). H, Quantitative analysis of the blood flow in the ischemic brain. Comparison of recovery from ischemia after 20m-MCAO between Wt and AM-Tg. MCA-Oc, blood flow during MCA occlusion; **, $P < 0.01$ for Wt *vs.* AM-Tg by ANCOVA; n = 8. I, Quantitative analysis of capillary density in the ischemic brain. Comparison of time course for increase in capillary density, determined as the number of PECAM-1$^+$ cells, between Wt and AM-Tg mice. *, $P < 0.05$; ns, not significant; n = 8.

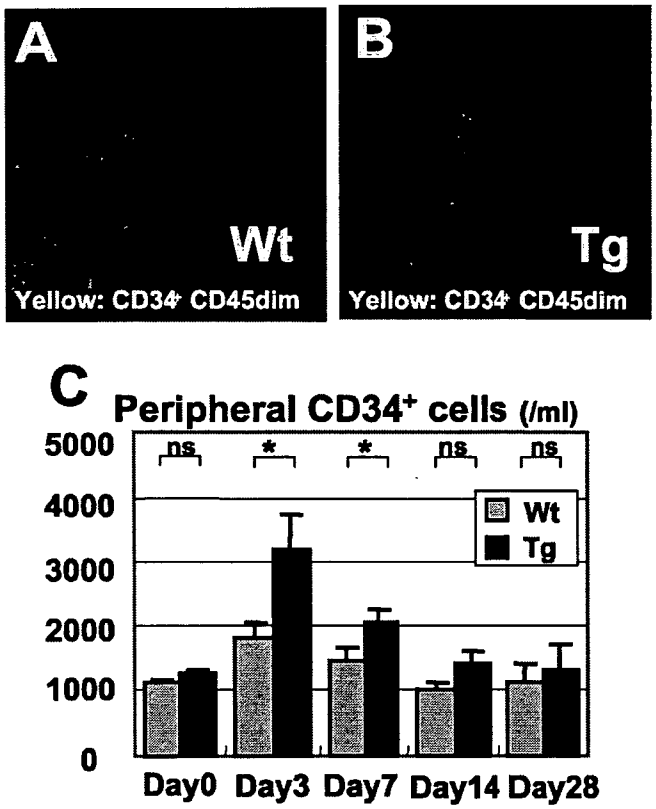

FIG. 5. Effects of AM on mobilization of $CD34^+$ mononuclear cells into peripheral blood after 20m-MCAO. A–C, Quantification of $CD34^+$ mononuclear cells after 20m-MCAO. Scatter plots for fluorescence-activated cell sorting analysis of the $CD34^+$ cells in peripheral blood of Wt (A) and AM-Tg (B) on postoperative d 3. *Yellow*, $CD34^+$-CD45dim mononuclear cells. Comparison of the time course for mobilization of $CD34^+$ cells into peripheral blood between Wt and AM-Tg (C). *, $P < 0.05$; ns, not significant; n = 6.

treatment. The result showed comparable levels of neuroprotection and vascular regeneration between the low-concentration line and the high-concentration line (Table 3). We further analyzed BP-matched mice by administration of low-dose hydralazine (0.1 mM in drinking water) to exclude the possibility that lower BP observed in AM-Tg mice caused beneficial effects after 20m-MCAO. As shown in Table 3, lower BP alone did not reduce the infarct area nor promote vascular regeneration, although hydralazine administration caused BP reduction comparable to that in AM-Tg mice.

Brain edema was reduced in AM-Tg mice at 24 h after 2 h MCAO

The survival rate of mice after the fatal stroke, 2 h-MCAO, was 0% on d 7. We observed no significant difference in the rate between Wt and AM-Tg mice. The edema volume was reduced in AM-Tg mice 24 h after 2 h-MCAO; although the infarct volume showed no significant difference between them. Edema volume (% volume of contralateral hemisphere) was 13.5 ± 1.2 in Wt *vs.* 9.7 ± 0.9 in AM-Tg ($P < 0.05$; n = 9, Fig. 7C), whereas infarct volume (% volume of contralateral hemisphere) was 39.0 ± 4.9 in Wt *vs.* 44.5 ± 7.3 in AM-Tg (not significant; n = 9; Fig. 7, A and B). As shown in Fig. 7D, we found that Evans Blue leakage into the ischemic

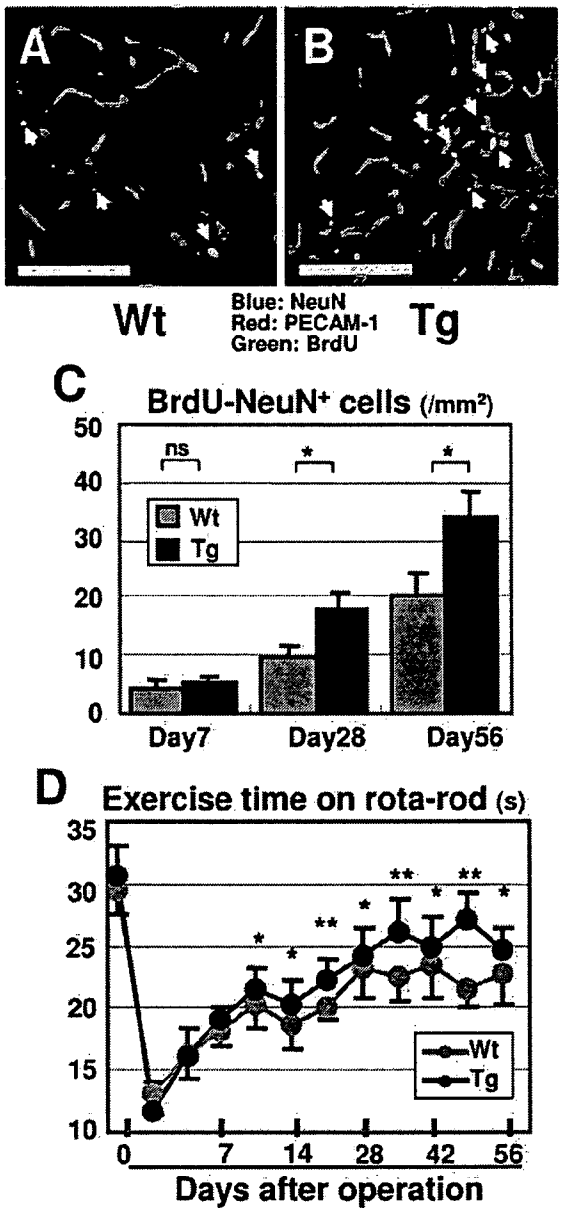

FIG. 6. Effects of AM on neurogenesis and recovery of impaired motor function after 20m-MCAO. A and B, Detection of regenerated neurons on postoperative d 56 by immunostaining for BrdU and NeuN. *Arrows*, BrdU-NeuN double-positive cells in the ischemic core of Wt (A) and AM-Tg (B). *Scale bar*, 100 μm. C, Quantitative analysis of regenerated neurons. *, $P < 0.05$; ns, not significant; n = 12. D, Recovery of impaired motor function after 20m-MCAO, quantified as the exercise time on an accelerating rota-rod from the start to collapse down. *, $P < 0.05$; **, $P < 0.01$ for Wt *vs.* AM-Tg by ANCOVA; n = 14.

core was significantly reduced in AM-Tg mice. The content of Evans Blue (ng/g tissue) in the ischemic brain at 24 h after 2 h-MCAO was 239.4 ± 37.3 in Wt *vs.* 133.9 ± 9.4 in AM-Tg ($P < 0.01$; n = 4; Fig. 7E).

AM exerted direct antiapoptotic and neurodifferentiating effects on neuronal cells in vitro

After 48 h incubation of NHNP under serum-free apoptotic conditions, in which the number of the cells had decreased

TABLE 2. Significant correlation between the regenerative elements and apoptosis, neurogenesis, and functional recovery after 20m-MCAO

X	Y	Regression line	*P*
Capillary density (% field)	Apoptotic cells (/mm^2)	Y = −2.3X+37	0.01
Capillary density (% field)	Regenerated neuron (/mm^2)	Y = 3.2X-21	0.003
Capillary density (% field)	Rota-rod result (sec)	Y = 1.3X+9	0.005
Regenerated neuron (/mm^2)	Rota-rod result (sec)	Y = 0.3X+19	0.08

n = 12–24.

to half, the viable cell number was increased in the AM 10^{-8} mol/liter-treated group to 38.8 ± 7.1% over the control ($P < 0.01$; n = 4; Fig. 8C). The ratio of ssDNA$^+$ cells to total cells (%) was 9.8 ± 1.9 in Wt *vs.* 4.0 ± 0.6 in the AM 10^{-8} mol/liter-treated group ($P < 0.05$; n = 4; Fig. 8, A, B, and D).

After 7-d incubation of PC12 cells under differentiation condition, both the cell number and the length of neuronal process increased dose dependently as a result of AM treatment ($P < 0.01$; n = 6; Fig. 8, E and I). Coculture with endothelial cells also increased the cell number and the length of neuronal process. The effect of AM was canceled by AM blockers, PKA inhibitors, and PI3K inhibitors (Table 4).

Exogenous administration of AM reduced infarct area, promoted vascular regeneration, and improved neurological function after 20m-MCAO

We further examined the effects of exogenous infusion of mature AM by means of an osmotic pump in the amount reported to achieve a plasma concentration of 2 fmol/ml. Implantation of the pump just after the operation resulted in increase in the blood flow and reduction of the infarct area on postoperative d 7 to a comparable level to those in AM-Tg mice. Moreover, the treatment started at 24 h after the operation (d 1) showed almost the same therapeutic effect. However, the implantation at 72 h after the operation (d 3) failed to reveal any significant effect (Fig. 9, A and B). The rota-rod exercise time was significantly improved in the AM-treated group. The exercise time (second) on d 7 was 17.0 ± 1.5 in vehicle group *vs.* 18.1 ± 2.0 in AM-treated group (n = 6 for vehicle group and 12 for AM-treated group; $P < 0.05$ by ANCOVA).

Discussion

In the present study, we generated novel transgenic mice that overproduce AM in their liver without overproduction of mature PAMP and investigated the roles of AM in degeneration or regeneration processes after brain ischemia, which can be defined as brain remodeling, as summarized in Fig. 10. Brain edema in acute phase, neuronal loss and gliosis in subacute to chronic phase after 20m-MCAO were reduced in AM-Tg mice. Furthermore, vascular regeneration, mobilization of CD34$^+$ mononuclear cells and subsequent neurogenesis were enhanced in them. These effects resulted in improved recovery of motor function after the nonfatal stroke. AM was also found to exert direct antiapoptotic and neuro-differentiating effects on neuronal cells *in vitro*. Exogenous administration of AM in mice after 20m-MCAO also

TABLE 3. Comparison of the effects on neuroprotection and vascular regeneration after 20m-MCAO between Wt control mice, hydralazine-administrated mice, and the low and high concentration lines of AM-Tg

Mice	Infarct area (mm^2/field)	Brain blood flow (% Contralateral)	Systolic BP (mm Hg)
Control	0.90 ± 0.09	80.8 ± 2.3	120.1 ± 2.2
Hydralazine	0.94 ± 0.17^{ns}	79.6 ± 2.6^{ns}	101.0 ± 3.9^a
Low-conc. AM-Tg	0.58 ± 0.12^b	88.4 ± 2.9^b	105.1 ± 1.8^a
High-conc. AM-Tg	0.67 ± 0.09^b	86.3 ± 2.0^b	106.4 ± 3.5^a

conc., Concentration.
$^a P < 0.01$; $^b P < 0.05$; ns, not significant *vs.* control; n = 6.

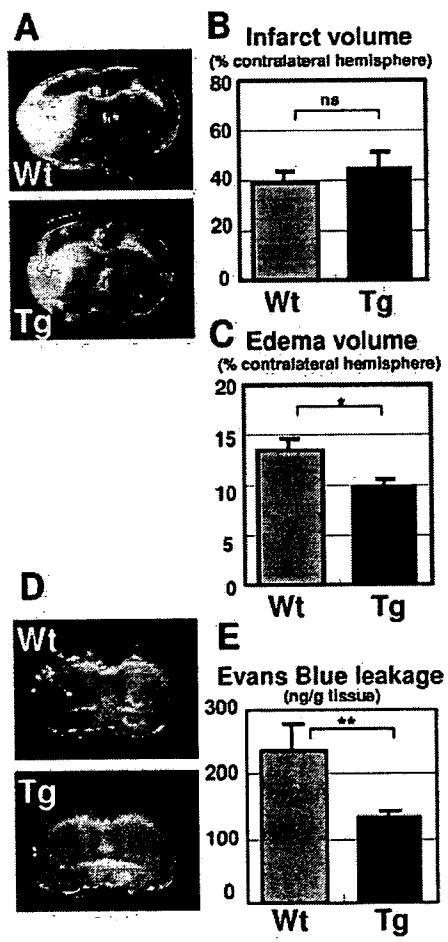

FIG. 7. Effects of AM on infarct size and brain edema in the fatal stroke, 2 h-MCAO. A, Comparison of infarct size between Wt and AM-Tg with 2,3,5-triphenyltetrazolium chloride staining at 4.0 mm from the frontal pole. *White area* represents infarction. B and C, Infarct (B) and edema (C) volumes quantified 24 h after the operation of 2 h-MCAO. *, $P < 0.05$; ns, not significant for Wt and AM-Tg; n = 9. D: Representative image of *in situ* Evans Blue leakage into the ischemic core at 24 h after 2 h-MCAO. E, Quantification of Evans Blue in the ischemic brain. **, $P < 0.01$; n = 4.

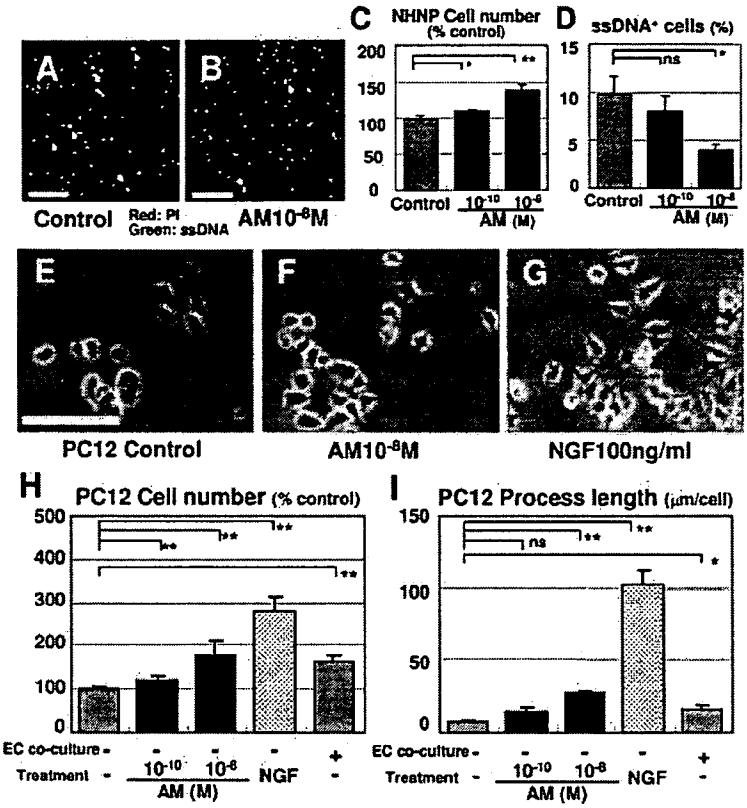

FIG. 8. Effects of AM *in vitro* on apoptosis of NHNP neuronal progenitor cells and neuronal differentiation of PC12 cells. A–D, *In vitro* analysis of apoptotic NHNP after incubation with (B) or without (A) AM. NHNP cell number (C) and the ratio of ssDNA$^+$ cells to total cells (D) after 48 h incubation. *, $P < 0.05$; **, $P < 0.01$; ns, not significant *vs.* control; n = 4; *scale bar*, 100 μm. E–G, Effects of AM on neuronal differentiation of PC12 cells evaluated by the length of neuronal process. Microscopic examination of PC12 cells after incubation for 7 d (E). AM (F) or nerve growth factor (G) was added to the culture medium. Quantification of cell number (H) and the length of neuronal process (I). *, $P < 0.05$; **, $P < 0.01$; ns, not significant; n = 6; *scale bar*, 100 μm.

reduced the infarct area, and promoted vascular regeneration and functional recovery.

Stroke causes two different types of neuronal death: necrosis and apoptosis. Acute neuronal loss, which is completed within a few days after ischemic damage, is necrotic, whereas delayed neuronal loss, which may start several days after transient ischemia, is considered to be apoptotic (27, 28). Many studies have found that treatments that reduce inflammation or oxidative stress are beneficial for the prevention of apoptotic neuronal loss (29, 30).

In this study, we demonstrated that AM exerts neuroprotective actions in the ischemic brain. A significant reduction in neuronal loss in AM-Tg mice after 20m-MCAO became obvious after postoperative d 7, but was not obvious before d 3. A significant decrease in ssDNA-positive cells inside and on the border of the ischemic area was observed in AM-Tg mice in association with a reduction in CD45$^+$ cells and *in situ* ROS production in the subacute phase. AM is therefore assumed to reduce delayed neuronal loss through suppression of the apoptotic process. Furthermore, we confirmed that AM directly suppresses apoptosis of neuronal progenitor cells *in vitro*. These findings suggest that AM exerts neuroprotective effects on the ischemic brain by reducing apoptotic neuronal loss through both its direct antiapoptotic action on neurons and indirect effect via antiinflammation and anti-ROS production. Consistent with the findings in this study, several recent reports have provided evidences for the organ-protective effects of AM against inflammation and oxidative stress (31–33). In addition, we found significant negative correlation between capillary density and apoptotic cells in the same section on postoperative d 7 after 20m-MCAO. Moreover, the infarct area kept expanding between d 7–28 in Wt mice, whereas AM-Tg mice did not show the increase in size in this period. These findings suggest that the increased blood flow in AM-Tg mice was one of the causes of neuroprotection after 20m-MCAO, although we suppose that multiple actions of AM, as described above, could also contribute for neuroprotection.

Increased vascularity is reported to be associated with improved neurological recovery in human patients with stroke (34). This implies that physiological vascular regeneration in the ischemic brain constitutes a beneficial response for the recovery of impaired neurological function. Moreover, neurogenesis after stroke even in adulthood has been demonstrated to occur in a place surrounded by the vascu-

TABLE 4. Effects of AM-antagonists, PKA inhibitors, and PI3K inhibitors on AM-induced neural differentiation of PC12 cells

	Process length (μm/cell)
PC12	6.8 ± 1.7
+AM (10^{-8} mol/liter)	23.6 ± 4.0[a]
+AM+AM(22–52) (10^{-5} mol/liter)	11.8 ± 3.4[b]
+AM+CGRP(8–37) (10^{-5} mol/liter)	14.8 ± 1.9[c]
+AM+Rp-cAMP (10^{-5} mol/liter)	10.2 ± 2.7[b]
+AM+PKA Inh (10^{-6} mol/liter)	7.2 ± 2.3[b]
+AM+LY294002 (10^{-5} mol/liter)	4.6 ± 1.6[b]
+AM+wortmannin (10^{-7} mol/liter)	5.4 ± 1.1[b]
PC12-EC coculture	20.7 ± 2.1[a]

EC, Endothelial cell.

[a] $P < 0.01$ *vs.* PC12 without AM; [b] $P < 0.01$ *vs.* PC12 with AM (10^{-8} mol/liter); [c] $P < 0.05$; n = 8.

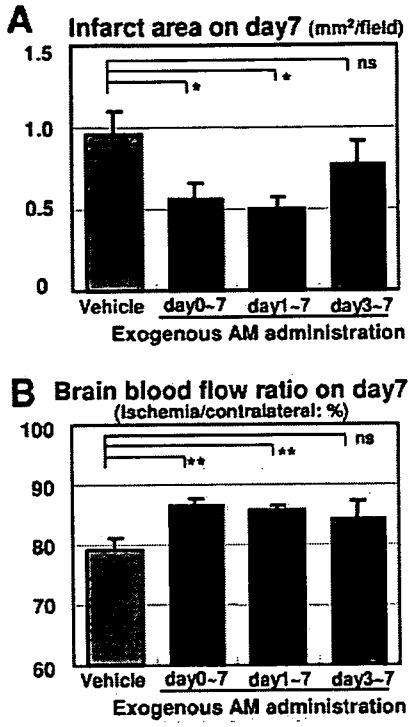

FIG. 9. Effects of exogenously administrated AM on neuroprotection and vascular regeneration after 20m-MCAO. 50 ng/h AM was administrated to mice with an ip implanted osmotic pump. Infarct area (A) and blood flow (B) on postoperative d 7 with different starting points for AM administration. *, $P < 0.05$; **, $P < 0.01$; ns, not significant *vs.* vehicle; n = 6.

lature, the so-called "vascular niche" (35), where endothelial cells secrete neurogenic factors, including basic fibroblast growth factor, vascular endothelial growth factor, and brain-derived neurotrophic factor, and create conditions conducive to neurogenesis (36). Therefore, vascular regeneration is assumed to rescue ischemic brain via not only supply of oxygen and nutrition but also promotion of neurogenesis. We confirmed in this study that neurogenesis occurred adjacent to neovessels in the ischemic core and the number of regenerated neurons was correlated with vascular density.

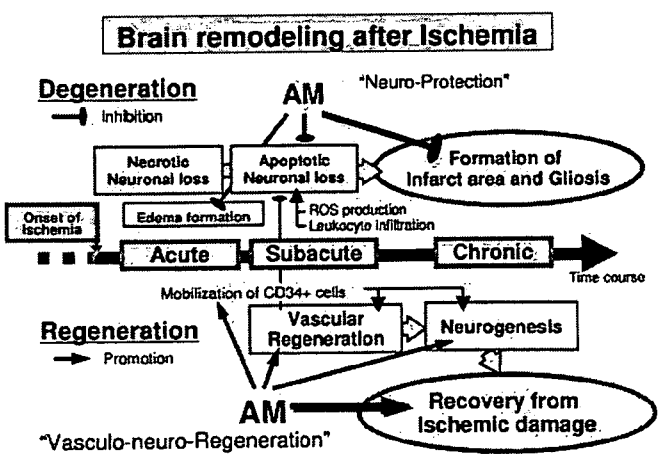

FIG. 10. Summary of brain remodeling after ischemia and effects of AM on the ischemic brain observed in this study.

We have assigned the term "vasculo-neuro-regeneration" to the entire process of enhancement of vasculogenesis and subsequent neurogenesis.

We demonstrated that AM promotes vasculo-neuro-regeneration in the ischemic brain. Blood flow and capillary density in the ischemic brain after 20m-MCAO was significantly enhanced in AM-Tg mice after postoperative d 7 with subsequent promotion of neurogenesis after d 28. The promoted vasculogenesis and neurogenesis observed in AM-Tg mice was significantly correlated with the functional recovery after 20m-MCAO. This result suggests that these two regenerative elements might contribute to the functional recovery after 20m-MCAO. The neovascularization was preceded by augmented mobilization of $CD34^+$ mononuclear cells, which are known to differentiate into endothelial cells and contribute to vasculogenesis (37). Recently, iv infusion of $CD34^+$ cells has reported to promote not only neovascularization but also neurogenesis (38). Furthermore, we observed the direct promoting action of AM on neural differentiation of PC12 cells via cAMP/PKA- and PI3K/Akt-dependent pathways. The totality of these findings suggests that the neurogenic action of AM *in vivo* comprises at least two different mechanisms: a direct action on neuronal cells through activation of PKA and Akt and an indirect action on neurogenesis after enhanced neovascularization.

Judging from the ratio of mature AM to total AM as shown in Table 1, the mature AM concentration in the ischemic brain of AM-Tg mice was expected to be 1~4 fmol/g tissue. The concentration seems to be comparable to the reported effective concentration of mature AM *in vivo* (25, 39). The *in vivo* concentration of human mature AM in the whole brain (1 fmol/g tissue level) and in the plasma (10 fmol/ml level) might be lower than the minimal concentration required for its *in vitro* action (100 fmol/ml) observed in this study. The actual effective concentration *in vitro*, however, might be lower because the administrated peptide is rapidly degradated *in vitro*. In addition, it is demonstrated in previous reports including ours (40, 41), that peptides could exert their significant actions at the stably maintained concentration, that is, by 2 orders of magnitude lower than that of bolus administration. In AM-Tg mice, the AM concentration was maintained at the same level due to the constitutive overproduction by the human serum amyloid P component promoter. Thus, we suppose that the direct neuronal action of AM *in vivo* could be possible in this stroke model.

In view of clinical application, we also tried exogenous administration of AM by ip implanted osmotic pump to determine appropriate amount and timing of AM administration after 20m-MCAO. Previous reports on AM administration for rodents or human set the therapeutic dose at 2~25 fmol/ml (25, 39). For our experiments, therefore, we used two lines of transgenic mice with a plasma concentration of mature AM of 24.9 ± 4.2 and 2.6 ± 0.6 fmol/ml. The results showed comparable effects of AM in these two lines on neuroprotection and vascular regeneration. This led us to conclude that a plasma level of 2~3 fmol/ml of mature AM, 3~5 times higher than its physiological concentration, was sufficient to attain therapeutic effects for the mice after 20m-MCAO. We next tried exogenous infusion of AM with an osmotic pump in the amount reported to achieve a plasma

concentration of 2~3 fmol/ml. The exogenous AM treatment which started just after the induction of 20m-MCAO or at 24 h after produced significant effects that were comparable to those seen in the two lines of AM-Tg mice. However, that from 72 h postoperatively failed to reveal significant effects. These results showed that appropriate timing to start AM administration after stroke is less than 72 h after the event.

We performed two different stroke models, nonfatal 20m-MCAO and fatal 2 h-MCAO. In 2 h-MCAO, we observed significant reduction of brain edema in AM-Tg mice through reduction of vascular permeability, which is compatible with previous report (42). However, infarct size was not reduced on postoperative d 1 after 2 h-MCAO. The result suggests that AM exerts more significant therapeutic effect on the brain tissue after nonfatal ischemia. The therapeutic potential for brain edema after fatal stroke is further to be elucidated.

Cerebral ischemia, including stroke, vascular Parkinson's disease and vascular dementia, is one of the most serious medical problems because it causes critical impairment of activity and quality of daily life. Regenerative medicine is now in the spotlight as a promising therapy to treat ischemic brain which has been considered to be irreversible and indicated for no active treatment. Various humoral factors are anticipated for their therapeutic potential for ischemic brain through neurogenic (*e.g.* basic fibroblast growth factor and epidermal growth factor) and angiogenic (*e.g.* vascular endothelial growth factor and hepatocyte growth factor) effects (43–47). Among them, we believe that the vascular hormone AM has several advantages as a therapeutic agent for ischemic brain. We can expect multiple effects of AM through its neuroprotective and vasculo-neuro-regenerative actions as shown in this study. In addition, AM has already been safely used for human patients with heart failure or pulmonary hypertension without any mention of critical adverse effects resulting from iv administration (39).

Thus, we are prompted to propose a new strategy to rescue ischemic brain by using vascular hormone AM for the combined neuroprotective and vasculo-neuro-regenerative therapy to improve impaired neurological function.

Acknowledgments

This work was supported by grants from Japanese ministry of Education, Culture, Sports, Science and Technology; ministry of Health, Labor and Welfare; and University of Kyoto 21st Century Centers of Excellence program. We thank Dr. Seiichi Hashida (Department of Biochemistry, University of Miyazaki) for measuring mature PAMP; and Dr. Kazuhiko Nozaki and Masaki Nishimura, (Department of Neurosurgery, University of Kyoto) for technical assistance.

Received August 15, 2005. Accepted December 19, 2005.

Address all correspondence and requests for reprints to: Hiroshi Itoh, M.D., Ph.D., Department of Medicine and Clinical Science, Kyoto University Graduate School of Medicine; 54 Shogoin Kawahara-cho, Sakyo-ku, Kyoto 606-8507, Japan. E-mail: hiito@kuhp.kyoto-u.ac.jp.

This work was supported by Japanese ministry of Education, Culture, Sports, Science and Technology; ministry of Health, Labor and Welfare; and University of Kyoto 21st Century Centers of Excellence program.

References

1. Kitamura K, Kangawa K, Kawamoto M, Ichiki Y, Nakamura S, Matsuo H, Eto T 1993 Adrenomedullin: a novel hypotensive peptide isolated from human pheochromocytoma. Biochem Biophys Res Commun 92:553–560
2. Nagaya N, Mori H, Murakami S, Kangawa K, Kitamura S 2005 Adrenomedullin: angiogenesis and gene therapy. Am J Physiol Regul Integr Comp Physiol 288:R1432–R1437
3. Shindo T, Kurihara Y, Nishimatsu H, Moriyama N, Kakoki M, Wang Y, Imai Y, Ebihara A, Kuwaki T, Ju KH, Minamino N, Kangawa K, Ishikawa T, Fukuda M, Akimoto Y, Kawakami H, Imai T, Morita H, Yazaki Y, Nagai R, Hirata Y, Kurihara H 2001 Vascular abnormalities and elevated blood pressure in mice lacking adrenomedullin gene. Circulation 104:1964–1971
4. Shimosawa T, Shibagaki Y, Ishibashi K, Kitamura K, Kangawa K, Kato S, Ando K, Fujita T 2002 Adrenomedullin, an endogenous peptide, counteracts cardiovascular damage. Circulation 105:106–111
5. Imai Y, Shindo T, Maemura K, Sata M, Saito Y, Kurihara Y, Akishita M, Osuga J, Ishibashi S, Tobe K, Morita H, Oh-hashi Y, Suzuki T, Maekawa H, Kangawa K, Minamino N, Yazaki Y, Nagai R, Kurihara H 2002 Resistance to neointimal hyperplasia and fatty streak formation in mice with adrenomedullin overexpression. Arterioscler Thromb Vasc Biol 22:1310–1315
6. Miyashita K, Itoh H, Sawada N, Fukunaga Y, Sone M, Yamahara K, Yurugi-Kobayashi T, Park K, Nakao K 2003 Adrenomedullin provokes endothelial Akt activation and promotes vascular regeneration both in vitro and in vivo. FEBS Lett 544:86–92
7. Miyashita K, Itoh H, Sawada N, Fukunaga Y, Sone M, Yamahara K, Yurugi T, Nakao K 2003 Adrenomedullin promotes proliferation and migration of cultured endothelial cells. Hypertens Res 26:S93–S98
8. Abe M, Sata M, Nishimatsu H, Nagata D, Suzuki E, Terauchi Y, Kadowaki T, Minamino N, Kangawa K, Matsuo H, Hirata Y, Nagai R 2003 Adrenomedullin augments collateral development in response to acute ischemia. Biochem Biophys Res Commun 306:10–15
9. Kim W, Moon SO, Sung MJ, Kim SH, Lee S, So JN, Park SK 2003 Angiogenic role of adrenomedullin through activation of Akt, mitogen-activated protein kinase, and focal adhesion kinase in endothelial cells. FASEB J 17:1937–1939
10. Tokunaga N, Nagaya N, Shirai M, Tanaka E, Ishibashi-Ueda H, Harada-Shiba M, Kanda M, Ito T, Shimizu W, Tabata Y, Uematsu M, Nishigami K, Sano S, Kangawa K, Mori H 2004 Adrenomedullin gene transfer induces therapeutic angiogenesis in a rabbit model of chronic hind limb ischemia: benefits of a novel nonviral vector, gelatin. Circulation 109:526–531
11. Iwase T, Nagaya N, Fujii T, Itoh T, Ishibashi-Ueda H, Yamagishi M, Miyatake K, Matsumoto T, Kitamura S, Kangawa K 2005 Adrenomedullin enhances angiogenic potency of bone marrow transplantation in a rat model of hindlimb ischemia. Circulation 111:356–362
12. Eto T 2001 A review of the biological properties and clinical implications of adrenomedullin and proadrenomedullin N-terminal 20 peptide (PAMP), hypotensive and vasodilating peptides. Peptides 22:1693–1711
13. Serrano J, Alonso D, Fernandez AP, Encinas JM, Lopez JC, Castro-Blanco S, Fernandez-Vizarra P, Richart A, Santacana M, Uttenthal LO, Bentura ML, Martinez-Murillo R, Martinez A, Cuttitta F, Rodrigo J 2002 Adrenomedullin in the central nervous system. Microsc Res Tech 57:76–90
14. Wang X, Yue TL, Barone FC, White RF, Clark RK, Willette RN, Sulpizio AC, Aiyar NV, Ruffolo Jr RR, Feuerstein GZ 1995 Discovery of adrenomedullin in rat ischemic cortex and evidence for its role in exacerbating focal brain ischemic damage. Proc Natl Acad Sci USA 92:11480–11484
15. Dogan A, Suzuki Y, Koketsu N, Osuka K, Saito K, Takayasu M, Shibuya M, Yoshida J 1997 Intravenous infusion of adrenomedullin and increase in regional cerebral blood flow and prevention of ischemic brain injury after middle cerebral artery occlusion in rats. J Cereb Blood Flow Metab 17:19–25
16. Watanabe K, Takayasu M, Noda A, Hara M, Takagi T, Suzuki Y, Yoshia J 2001 Adrenomedullin reduces ischemic brain injury after transient middle cerebral artery occlusion in rats. Acta Neurochir (Wien) 143:1157–1161
17. Xia CF, Yin H, Borlongan CV, Chao J, Chao L 2004 Adrenomedullin gene delivery protects against cerebral ischemic injury by promoting astrocyte migration and survival. Hum Gene Ther 15:1243–1254
18. Hashida S, Kitamura K, Nagatomo Y, Shibata Y, Imamura T, Yamada K, Fujimoto S, Kato J, Morishita K, Eto T 2004 Development of an ultrasensitive enzyme immunoassay for human proadrenomedullin N-terminal 20 peptide and direct measurement of two molecular forms of PAMP in plasma from healthy subjects and patients with cardiovascular disease. Clin Biochem 37:14–21
19. Longa EZ, Weinstein PR, Carlson S, Cummins R 1989 Reversible middle cerebral artery occlusion without craniectomy in rats. Stroke 20:84–91
20. Teramoto T, Qiu J, Plumier JC, Moskowitz MA 2003 EGF amplifies the replacement of parvalbumin-expressing striatal interneurons after ischemia. J Clin Invest 111:1125–1132
21. Venditti A, Battaglia A, Del Poeta G, Buccisano F, Maurillo L, Tamburini A, Del Moro B, Epiceno AM, Martiradonna M, Caravita T, Santinelli S, Adorno G, Picardi A, Zinno F, Lanti A, Bruno A, Suppo G, Franchi A, Franconi G, Amadori S 1999 Enumeration of CD34+ hematopoietic progenitor cells for clinical transplantation: comparison of three different methods. Bone Marrow Transplant 24:1019–1027
22. Swanson RA, Morton MT, Tsao-Wu G, Savalos RA, Davidson C, Sharp FR 1990 A semiautomated method for measuring brain infarct volume. J Cereb Blood Flow Metab 10:290–293
23. Zhang ZG, Zhang L, Croll SD, Chopp M 2002 Angiopoietin-1 reduces cerebral blood vessel leakage and ischemic lesion volume after focal cerebral embolic ischemia in mice. Neuroscience 2002 113:683–687

24. Hayashi H, Ishisaki A, Imamura T 2003 Smad mediates BMP-2-induced upregulation of FGF-evoked PC12 cell differentiation. FEBS Lett 536:30–34
25. Iimuro S, Shindo T, Moriyama N, Amaki T, Niu P, Takeda N, Iwata H, Zhang Y, Ebihara A, Nagai R 2004 Angiogenic effects of adrenomedullin in ischemia and tumor growth. Circ Res 95:415–423
26. Nakano S, Kogure K, Fujikura H 1990 Ischemia-induced slowly progressive neuronal damage in the rat brain. Neuroscience 38:115–124
27. Graham SH, Chen J 2001 Programmed cell death in cerebral ischemia. J Cereb Blood Flow Metab 21:99–109
28. Northington FJ, Ferriero DM, Graham EM, Traystman RJ, Martin LJ 2001 Early neurodegeneration after hypoxia-ischemia in neonatal rat is necrosis while delayed neuronal death is apoptosis. Neurobiol Dis 8:207–219
29. Stoll G, Jander S, Schroeter M 1998 Inflammation and glial responses in ischemic brain lesions. Prog Neurobiol 56:149–171
30. Gilgun-Sherki Y, Rosenbaum Z, Melamed E, Offen D 2002 Antioxidant therapy in acute central nervous system injury: current state. Pharmacol Rev 54:271–284
31. Kim W, Moon SO, Lee S, Sung MJ, Kim SH, Park SK 2003 Adrenomedullin reduces VEGF-induced endothelial adhesion molecules and adhesiveness through a phosphatidylinositol 3′-kinase pathway. Arterioscler Thromb Vasc Biol 23:1377–1383
32. Kawai J, Ando K, Tojo A, Shimosawa T, Takahashi K, Onozato ML, Yamasaki M, Ogita T, Nakaoka T, Fujita T 2004 Endogenous adrenomedullin protects against vascular response to injury in mice. Circulation 109:1147–1153
33. Niu P, Shindo T, Iwata H, Iimuro S, Takeda N, Zhang Y, Ebihara A, Suematsu Y, Kangawa K, Hirata Y, Nagai R 2004 Protective effects of endogenous adrenomedullin on cardiac hypertrophy, fibrosis, and renal damage. Circulation 109:1789–1794
34. Krupinski J, Kaluza J, Kumar P, Kumar S, Wang JM 1994 Role of angiogenesis in patients with cerebral ischemic stroke. Stroke 25:1794–1798
35. Palmer TD, Willhoite AR, Gage FH 2000 Vascular niche for adult hippocampal neurogenesis. J Comp Neurol 425:479–494
36. Louissaint Jr A, Rao S, Leventhal C, Goldman SA 2002 Coordinated interaction of neurogenesis and angiogenesis in the adult songbird brain. Neuron 34:945–960
37. Asahara T, Murohara T, Sullivan A, Silver M, van der Zee R, Li T, Witzenbichler B, Schatteman G, Isner JM 1997 Isolation of putative progenitor endothelial cells for angiogenesis. Science 275:964–967
38. Taguchi A, Soma T, Tanaka H, Kanda T, Nishimura H, Yoshikawa H, Tsukamoto Y, Iso H, Fujimori Y, Stern DM, Naritomi H, Matsuyama T 2004 Administration of CD34+ cells after stroke enhances neurogenesis via angiogenesis in a mouse model. J Clin Invest 114:330–338
39. Nagaya N, Satoh T, Nishikimi T, Uematsu M, Furuichi S, Sakamaki F, Oya H, Kyotani S, Nakanishi N, Goto Y, Masuda Y, Miyatake K, Kangawa K 2000 Hemodynamic, renal, and hormonal effects of adrenomedullin infusion in patients with congestive heart failure. Circulation 101:498–503
40. Doi K, Itoh H, Ikeda T, Hosoda K, Ogawa Y, Igaki T, Yamashita J, Chun TH, Inoue M, Masatsugu K, Matsuda K, Ohmori K, Nakao K 1997 Adenovirus-mediated gene transfer of C-type natriuretic peptide causes G1 growth inhibition of cultured vascular smooth muscle cells. Biochem Biophys Res Commun 239:889–894
41. Komatsu Y, Itoh H, Suga S, Ogawa Y, Hama N, Kishimoto I, Nakagawa O, Igaki T, Doi K, Yoshimasa T, Nakao K 1996 Regulation of endothelial production of C-type natriuretic peptide in coculture with vascular smooth muscle cells. Role of the vascular natriuretic peptide system in vascular growth inhibition. Circ Res 78:606–614
42. Hippenstiel S, Witzenrath M, Schmeck B, Hocke A, Krisp M, Krull M, Seybold J, Seeger W, Rascher W, Schutte H, Suttorp N 2002 Adrenomedullin reduces endothelial hyperpermeability. Circ Res 91:618–625
43. Nakatomi H, Kuriu T, Okabe S, Yamamoto S, Hatano O, Kawahara N, Tamura A, Kirino T, Nakafuku M 2002 Regeneration of hippocampal pyramidal neurons after ischemic brain injury by recruitment of endogenous neural progenitors. Cell 110:429–441
44. Zhang ZG, Zhang L, Jiang Q, Zhang R, Davies K, Powers C, Bruggen N, Chopp M 2000 VEGF enhances angiogenesis and promotes blood-brain barrier leakage in the ischemic brain. J Clin Invest 106:829–838
45. Shimamura M, Sato N, Oshima K, Aoki M, Kurinami H, Waguri S, Uchiyama Y, Ogihara T, Kaneda Y, Morishita R 2004 Novel therapeutic strategy to treat brain ischemia: overexpression of hepatocyte growth factor gene reduced ischemic injury without cerebral edema in rat model. Circulation 109:424–431
46. Sun Y, Jin K, Xie L, Childs J, Mao XO, Logvinova A, Greenberg DA 2003 VEGF-induced neuroprotection, neurogenesis, and angiogenesis after focal cerebral ischemia. J Clin Invest 111:1843–1851
47. Sondell M, Lundborg G, Kanje M 1999 Vascular endothelial growth factor has neurotrophic activity and stimulates axonal outgrowth, enhancing cell survival and Schwann cell proliferation in the peripheral nervous system. J Neurosci 19:5731–5740

Endocrinology **is published monthly by The Endocrine Society (http://www.endo-society.org), the foremost professional society serving the endocrine community.**

FEBS Letters 581 (2007) 349–354

Augmentation of 11β-hydroxysteroid dehydrogenase type 1 in LPS-activated J774.1 macrophages – Role of 11β-HSD1 in pro-inflammatory properties in macrophages

Takako Ishii, Hiroaki Masuzaki*, Tomohiro Tanaka, Naoki Arai, Shintaro Yasue, Nozomi Kobayashi, Tsutomu Tomita, Michio Noguchi, Junji Fujikura, Ken Ebihara, Kiminori Hosoda, Kazuwa Nakao

Division of Endocrinology and Metabolism, Department of Medicine and Clinical Science, Kyoto University Graduate School of Medicine, 54, Shogoin Kawaharacho, Sakyoku, Kyoto 606-8507, Japan

Received 25 September 2006; revised 3 November 2006; accepted 13 November 2006

Available online 27 November 2006

Edited by Beat Imhof

Abstract Macrophage infiltration in obese adipose tissue provokes local inflammation and insulin resistance. Evidence has accumulated that activation of 11β-HSD1 in adipocytes is critically involved in dysfunction of adipose tissue. However, the potential role of 11β-HSD1 in macrophages still remains unclear. We here demonstrate that a murine macrophage cell line, J774.1 cells expressed 11β-HSD1 mRNA and reductase activity, both of which were augmented by lipopolysaccharide (LPS)-induced cell activation. Three kinds of pharmacological inhibition of 11β-HSD1 in LPS-treated macrophages significantly suppressed the expression and secretion of interleukin 1β, tumor necrosis factor α or monocyte chemoattractant protein 1, thereby highlighting a novel role of 11β-HSD1 in pro-inflammatory properties of activated macrophages.

Keywords: 11β-HSD1; Macrophage; Inflammation; Metabolic syndrome; Inhibitor; Adipocyte

1. Introduction

Functional abnormalities in adipose tissue have been implicated in the central pathophysiology of the metabolic syndrome [1]. Glucocorticoids regulate adipocyte differentiation, function and distribution, and in excess, cause visceral fat obesity and convergence of metabolic diseases [2]. Two iso-enzymes of 11β-HSD, 11β-HSD1 and 11β-HSD2 catalyze the interconversion between hormonally active cortisol and inactive cortisone within cells. 11β-HSD1 is abundantly expressed in adipose tissue and liver [2,3] and reactivates cortisol from cortisone (oxo-reductase) [4]. Previous reports have demonstrated that 11β-HSD1 predominates in adipocytes compared to 11β-HSD2 [2], which inactivates cortisol to cortisone (dehydrogenase). Targeted overexpression of 11β-HSD1 selectively in adipose tissue in mice exemplified metabolic derangements including visceral fat obesity, insulin resistance, dyslipidemia and hypertension [5,6]. Conversely, systemic 11β-HSD1 knockouts as well as adipose-specific 11β-HSD2 overexpressors are completely protected against metabolic diseases under overnutrition [7–9]. These data suggest that increased level of adipose 11β-HSD1 plays a crucial role in dysfunction of adipose tissue and resultant metabolic disorders.

On the other hand, recent studies have demonstrated that infiltration of macrophages in obese adipose tissue provokes local and systemic inflammation and insulin resistance [10–12]. It has been shown that matured adipocytes abundantly express 11β-HSD1 which is critically involved in dysfunction of adipose tissue [2,5]. However, the potential role of 11β-HSD1 in macrophages remains largely unclear. In this context, we explored the expression and regulation of 11β-HSD1 in a murine reticular cell sarcoma-derived J774.1 macrophages [13]. To our knowledge, this is the first to demonstrate that 11β-HSD1 is critically involved in pro-inflammatory properties of activated macrophages.

*Corresponding author. Fax: +81 75 771 9452.
E-mail address: hiroaki@kuhp.kyoto-u.ac.jp (H. Masuzaki).

Abbreviations: 11β-HSD1, 11β-hydroxysteroid dehydrogenase type 1; 11β-HSD2, 11β-hydroxysteroid dehydrogenase type 2; LPS, lipopolysaccharide; TLR4, toll-like receptor 4; IL-1β, interleukin 1β; IL1R1, interleukin 1 receptor type 1; TNF-α, tumor necrosis factor α; TNFR1, tumor necrosis factor receptor type 1; MCP-1, monocyte chemoattractant protein 1; CCR2, chemokine (C–C motif) receptor 2; GR, glucocorticoid receptor; SVF, stromal-vascular fraction; inhibitor A, 3-(1-adamantyl)-5,6,7,8,9,10-hexahydro[1,2,4]triazolo[4,3-α]azocine trifluoroacetate salt; inhibitor B(BVT-3498), 2,4,6-trichloro-*N*-(5,5-dimethyl-7-oxo-4,5,6,7-tetrahydro-1,3-benzothiazol-2-yl)benzenesulfonamide; CBX, carbenoxolone; DEX, dexamethasone

2. Materials and methods

2.1. Reagents and chemicals

All reagents were of analytical grade unless otherwise indicated. Carbenoxolone [4,14,15], a non-selective inhibitor for 11β-HSD1 and 11β-HSD2 was obtained from Sigma (St. Louis, MO, USA). Recently-developed 11β-HSD1 selective inhibitors, 3-(1-adamantyl)-5,6,7,8,9,10-hexahydro[1,2,4] triazolo [4,3-α] azocine trifluoroacetate salt (WO03/065983, Merck Co., USA) (inhibitor A for short, unless otherwise indicated) [16] and 2,4,6-trichloro-*N*-(5,5-dimethyl-7-oxo-4,5,6,7-tetrahydro-1,3-benzothiazol-2-yl) benzenesulfonamide (BVT-3498, Biovitrum, Sweden) (inhibitor B for short, unless otherwise indicated) [17,18] were synthesized according to the patent information.

0014-5793/$32.00
doi:10.1016/j.febslet.2006.11.032

2.2. Cell culture

Mouse reticulum cell sarcoma-derived J774.1 cells [13] were obtained from Cell Resource Center for Biomedical Research Institute of Development, Aging and Cancer, Tohoku University, Japan. Cells were cultured in RPMI 1640 plus 10% heat-inactivated FBS at 37 °C in 5% CO_2.

2.3. Quantitative real time PCR

Total RNA was extracted using Trizol Reagent (Invitrogen, USA) and cDNA was synthesized using iScript™ cDNA Synthesis Kit (Bio-Rad, USA) according to the manufacturer's instruction. The sequence of probes and primers are summarized in Table 1. Taqman PCR was performed using ABI Prism 7700 Sequence Detection System as instructed by the manufacture (Applied Biosystems, USA). Level of mRNA was normalized to those of 18S mRNA.

2.4. 11β-HSD1 enzyme activity assay

11β-HSD1 primarily acts as a reductase and reactivates cortisol from cortisone in viable cells. On the other hand, under some conditions such as tissue homogenate or microsome fraction, 11β-HSD1 acts as a dehydrogenase and inactivate cortisone to cortisol [2]. 11β-HSD1 reductase activity in intact cells was measured as reported [2]. Briefly, cells were incubated for 24 h in serum-free RPMI 1640, adding 250 nM cortisone including tritium labeled tracer [1,2-^{3}H]$_2$ cortisone for reductase activity and 250 nM cortisol with [1,2,6,7-^{3}H]$_4$ cortisol for dehydrogenase activity. Cortisol and cortisone were extracted using ethyl acetate, evaporated and resuspended in ethanol, separated by thin-layer chromatography in chloroform:methanol (95:5) and quantified by autoradiography.

To validate inhibitory potency of compounds against 11β-HSD1, using FreeStyle 293 cells transiently transfected with human 11β-HSD1, the enzyme activity assay was carried out with 20 mM Tris–HCl, pH 7.0, 50 μM NADPH, 5 μg protein of microsomal fraction, 300 nM ^{3}H-cortison for 2 h. The reaction was stopped by 18β-Glycyrrhetinic acid. The labeled cortisol product was captured by mouse monoclonal anti-cortisol antibody, bound to SPA beads coated with protein A, and quantified in a scintillation counter.

2.5. Measurement of IL-1β, TNF-α and MCP-1 concentrations in cultured media

Interleukin 1β (IL-1β), tumor necrosis factor α (TNF-α) and monocyte chemoattractant protein 1 (MCP-1) concentrations in J774.1 cell (1×10^6 cells/ml) cultured media were measured by enzyme-linked immunosorbent assay (ELISA) kits according to the manufacturers instructions (R&D Systems, USA).

2.6. Statistical analysis

Data are expressed as the means ± S.E.M. of triplicate experiments. Data were analyzed using one-way analysis of variance (ANOVA), followed by Student's *t*-tests for each pair for multiple comparisons. Differences were considered significant if $P < 0.05$.

3. Results

3.1. 11β-HSD1 mRNA level and reductase activity were substantially increased in activated J774.1 macrophages

Lipopolysaccharide (LPS) is a potent ligand for toll-like receptor (TLR) 4 and a representative activator of macrophages [19,20]. When J774.1 cells were treated with LPS (100 ng/ml) for 24 h, mRNA level of IL-1β, TNF-α and MCP-1 was markedly increased compared to control (approximately 1500-fold, 3-fold, 220-fold, respectively, $P < 0.01$). LPS (100 ng/ml, 24 h) also substantially augmented 11β-HSD1 mRNA level in J774.1 macrophages (~20-fold vs. control. $P < 0.01$) (Fig. 1A). 11β-HSD1 reductase activity was concomitantly augmented by LPS (100 ng/ml) compared to LPS-free control (2.9 ± 1.2-fold vs. control. $P < 0.05$) (Fig. 1B). Notably, 11β-HSD1 dehydrogenase activity was under-detectable not only at the basal but with LPS treatment (Fig. 1C).

3.2. Effect of pharmacological inhibition of 11β-HSD1 on inflammatory properties in J774.1 macrophages

To explore the potential role of 11β-HSD1 in cytokine release from activated macrophages, we examined the effect of pharmacological inhibition of 11β-HSD1 on gene expression of LPS-treated J774.1 cells. In the present study, two

Table 1
Sequences of TaqMan primers and probes

Gene	GenBank accession no.	Probe (FAM-5′ → 3′-TAMRA)	Primer (5′ → 3′)
Hsd11b1	NM008288	TCCGAGTTCAAGGCAGCGAGACACTACC	f CCAGGTCGGAGGAAGGTCTC r CCAGCAATGTAGTGAGCAGAGG
Hsd11b2	NM008289	TCAAGCCTGGCTGCTCCAAGACAG	f TCCCTGGGGTATCAAGGTCAG r CTCCCAGAGGTTCACATTAGTCAC
Il1b	NM008361	CATGGCACATTCTGTTCAAAGAGAGCCTG	f TCGCTCAGGGTCACAAAGAAA r CCATCAGAGGCAAGGAGGAA
Tnf	NM013693	CCCGACTACGTGCTCCTCACCCA	f TCTCTTCAAGGGACAAGGCTG r ATAGCAAATCGGCTGACGGT
Ccl2	NM011333	CCCCACTCACCTGCTGCTACTCATTCA	f TTGGCTCAGCCAGATGCA r CCAGCCTACTCATTGGGATCA
Il1r1	NM008362	CCTGACTTCAAGAATTACCTCATCGG	f GCATGTGCAGTTAATATACC r CAATTGTAGCCGTGAGGATG
Tnfrsf1a	NM011609	AGTGAGTGCGTCCCTTGCAGCC	f GCAGGGTTCTTTCTGAGAG r GGCACAACTTCATACACTCC
Ccr2	NM009915	CTCTGTCACCTGCATGGCCTGGTCT	f ATGAGTAACTGTGTGATTGACAAGCA r GCAGCAGTGTGTCATTCCAAGA
Nr3c1	NM008173	CCTGCTATGCTTTGCTCCTGATCTGATT	f ATCATACAGACAAGCAAGTGGAA r AGGGTAGAGTCATTCTCTGCTC
Tlr4	NM021297	CATGCCTTGTCTTCAATTGTTTCAA	f CTTCAGTGGCTGGATTTATC r GAGGTGGTGTAAGCCATG

Forward primers are designated by f and reverse primers by r.

Abbreviations: FAM, 6-carboxyfluorescein; TAMRA, 6-carboxytetramethylrhodamine. Hsd11b1, hydroxysteroid 11-beta dehydrogenase 1; *Hsd11b2*, hydroxysteroid 11-beta dehydrogenase 2; *Il6*, interleukin 1 beta; *Tnf*, tumor necrosis factor; *Ccl2* (=monocyte chemoattractant protein:MCP-1); chemokine (C–C motif) ligand 2, *Il1r1*; interleukin 1 receptor, type I, *Tnfrsf1a* (=TNFR1), tumor necrosis factor receptor superfamily member 1a; Ccr2, chemokine (C–C motif) receptor 2; *Nr3c1* (=glucocorcoid receptor, GR); nuclear receptor subfamily 3, group C, member 1; *Tlr4*, toll-like receptor 4.

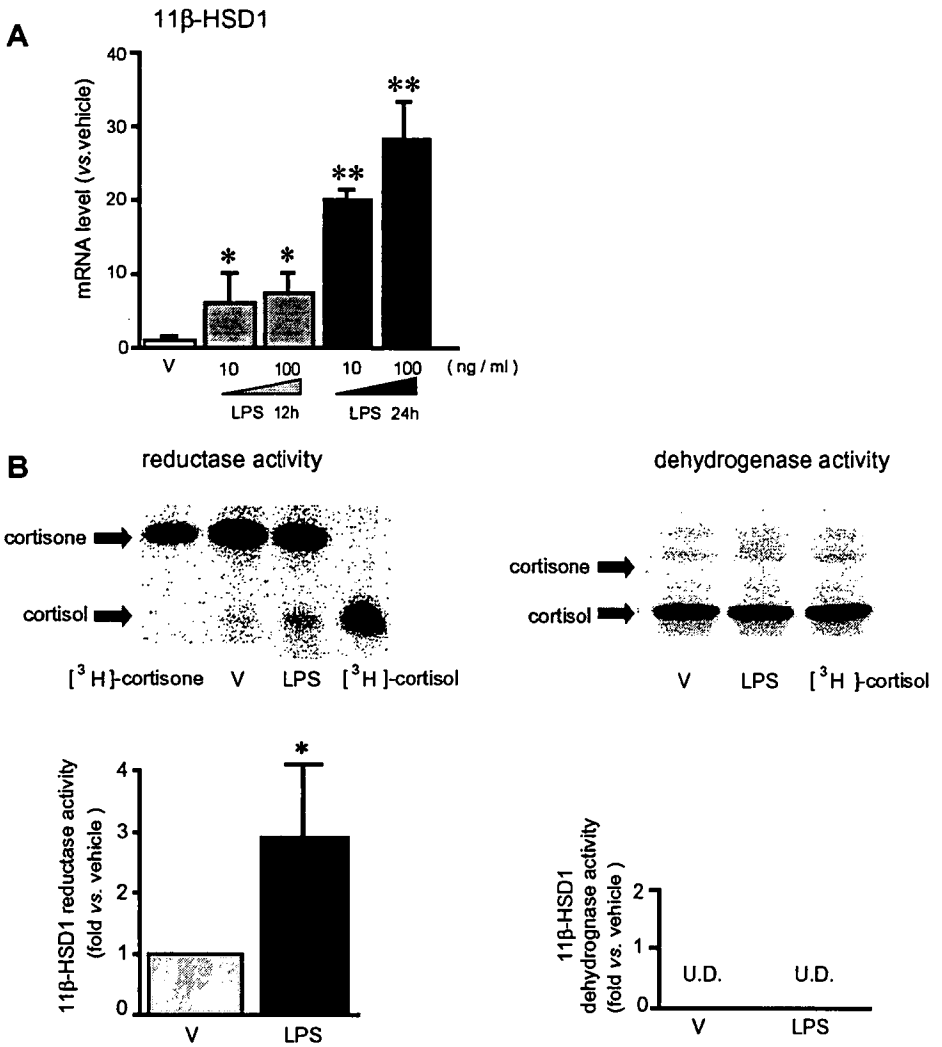

Fig. 1. 11β-HSD1 mRNA expression and reductase activity were induced by LPS in J774.1 macrophages. J774.1 cells (1×10^6 cells/ml, not-confluent) were treated with LPS ($10–10^3$ ng/ml, 12 or 24 h). (A) Level of mRNA for 11β-HSD1 was determined by real-time PCR. Level of each mRNA was normalized to that of 18S rRNA. (B) (left): 11β-HSD1 reductase activity (expressed as conversion ability of cortisone to cortisol) and (right): 11β-HSD1 dehydrogenase activity (expressed as conversion ability of cortisol to cortisone) were assessed in the media of J774.1 cells treated with 10 ng/ml LPS for 24 h. Reference corresponds to [^{3}H] cortisone or [^{3}H] cortisol used as a size marker. A representative autoradiograph of thin-layer chromatography (TLC) in 11β-HSD activity assay (upper) and quantification (lower). Intensities of signals at cortisol and cortisone correspond to the enzyme activity of reductase and dehydrogenase, respectively. U.D.; under detectable. Data are expressed as mean ± S.E.M. of triplicate experiments. $^*P < 0.05$ vs. vehicle (V) treated group.

kinds of 11β-HSD1 selective inhibitors: inhibitor A and inhibitor B were synthesized and employed (as mentioned in materials and methods). 11β-HSD1 and 11β-HSD2 non-selective inhibitor, carbenoxolone (CBX) was also utilized. Based on our data that 11β-HSD2 mRNA (data not shown) and corresponding enzyme activity (dehydrogenase) [2,3] were under detectable in J774.1 cells even with LPS treatment (Fig. 1), CBX was considered to act virtually as a specific inhibitor against 11β-HSD1.

In the microsome fraction assay, we verified that inhibitor A (100 μM), inhibitor B (100 μM) and CBX (1 μM), all potently inhibited 11β-HSD1 activity as little as 25% vs. control, respectively (Fig. 2A). In J774.1 cells, treatment of inhibitor A (10 μM), inhibitor B (100 μM), and CBX (100 μM) markedly inhibited 11β-HSD1 activity (48 ± 23% [$P < 0.05$], 30 ± 1% [$P < 0.01$], and 80 ± 7% [$P < 0.01$] of reduction vs. LPS-treated cells, respectively), confirming that these compounds serve as potent inhibitors against 11β-HSD1 in J774.1 cells (Fig. 2B).

Noteworthy is that treatment of J774.1 cells with inhibitor A (10 μM), inhibitor B (100 μM) and CBX (100 μM) reduced IL-1β mRNA level (27 ± 5%, 38 ± 10%, 88 ± 2% of reduction vs. LPS-treated cells without compounds, respectively, $P < 0.01$) (Fig. 3A, upper). Consequently, IL-1β concentration in the media was markedly decreased (inhibitor A; 34 ± 10%, CBX; 75 ± 3% of reduction vs. LPS-treated cells, respectively, $P < 0.01$) (Fig. 3A, lower). TNF-α mRNA (inhibitor B; 20 ± 11.7% [$P < 0.05$], CBX; 34 ± 5% [$P < 0.01$] of reduction vs. LPS-treated cells, respectively) (Fig. 3B, upper) and its concentration in the media (inhibitor B: 41 ± 8%, CBX: 57 ± 4% of reduction vs. LPS-treated cells, respectively, $P < 0.01$) (Fig. 3B, lower) were also significantly suppressed by the treatment of 11β-HSD1 inhibitors. In MCP-1, only CBX exerted

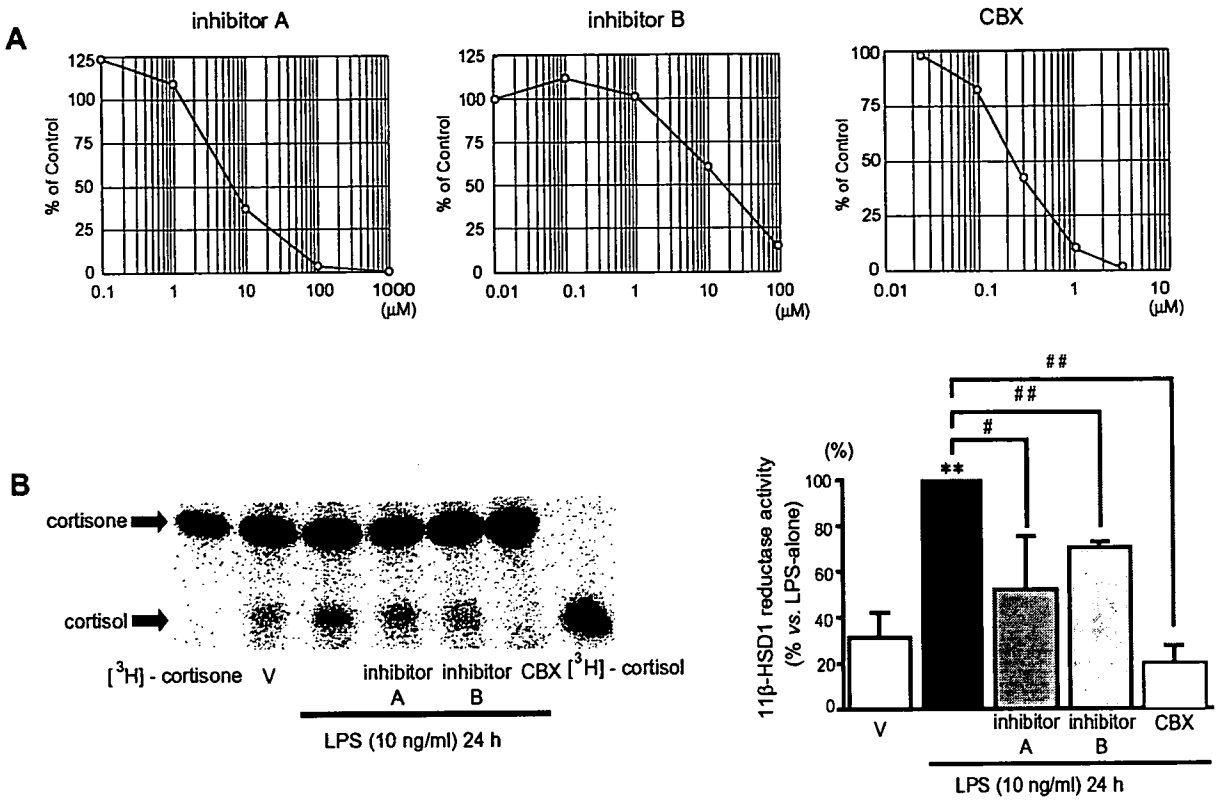

Fig. 2. 11β-HSD1 activity assay for validation of 11β-HSD1 inhibitors. (A) Microsome fraction 11β-HSD1 activity assay: inhibitor A (0.01–100 μM), inhibitor B (0.1–100 μM), CBX, carbenoxolone (0.01–10 μM). The *x*-axis shows the log concentration of each inhibitor and the *y*-axis shows log% inhibition of 11β-HSD1 activity compared to control. (B) Intact cell assay for 11β-HSD1 reductase activity. J774.1 cells were incubated for 24 h in serum-free RPMI 1640, adding 250 nM of cortisone with tritium labeled cortisone (left): a representative autoradiograph of TLC in 11β-HSD activity assay and (right): quantification of 11β-HSD activities. Intensities of signals at cortisol correspond to the enzyme activity of reductase. The *y*-axis shows the percentage of 11β-HSD1 reductase activity compared to LPS (10 mg/ml) treated cells per se. Treatment of inhibitor A (10 μM), inhibitor B (100 μM), and CBX (100 μM) substantially reduced 11β-HSD1 activity in J774.1 cells (inhibitor A and inhibitor B as mentioned in Section 2).

significant effect on the mRNA level (48 ± 11% of reduction vs. LPS-treated cells. $P < 0.01$) (Fig. 3C, upper) and concentration in the media (57 ± 4% of reduction vs. LPS-treated cells. $P < 0.01$) (Fig. 3C, lower).

The mRNA level of IL1R1 (receptor for IL-1β), TNFR1 (receptor for TNF-α), CCR2 (receptor for MCP-1), toll-like receptor 4 (TLR4) (receptor for LPS) and GR (receptor for glucocorticoid) was not significantly changed with these 11β-HSD1 inhibitors (data not shown).

3.3. Effect of dexamethasone on inflammatory properties in J774.1 macrophages

We examined the effect of glucocorticoid replenishment on the secretion of pro-inflammatory cytokine and chemokine in J774.1 macrophages. Treatment of J774.1 cells with dexamethasone (DEX) (10^{-10}–10^{-7} M, 24 h) suppressed the mRNA expression and secretion of IL-1β, TNFα and MCP-1 in a dose-dependent manner (supplementary figure A–F). Furthermore, co-treatment of LPS (10 ng/ml) with DEX markedly reduced the expression and secretion of IL-1β, TNFα and MCP-1 dose-dependently (supplementary figure A–F).

Treatment of J774.1 cells with DEX (10^{-7} M) reduced IL-1β mRNA level (85 ± 8% of reduction vs. vehicle, 91 ± 0.1% of reduction vs. LPS-treated cells, respectively, $P < 0.01$). Consequently, IL-1β concentration in the media was decreased (83 ± 8% of reduction vs. LPS-treated cells, $P < 0.01$) (supplementary figure A, D). Regarding TNF-α, mRNA (55 ± 8% of reduction vs. vehicle, 47 ± 14% of reduction vs. LPS-treated cells, respectively, $P < 0.01$) and concentration in the media (51 ± 14% of reduction vs. vehicle, 43 ± 8% of reduction vs. LPS-treated cells, respectively, $P < 0.01$) were markedly suppressed by DEX (supplementary figure B, E). Regarding MCP-1, DEX also decreased the mRNA level (65 ± 4% of reduction vs. vehicle [$P < 0.05$], 83 ± 3% of reduction vs. LPS-treated cells [$P < 0.01$], respectively) and concentration in the media (81 ± 10% of reduction vs. vehicle, 68 ± 5% of reduction vs. LPS-treated cells, respectively, $P < 0.01$) (supplementary figure C, F).

4. Discussion

Here, we demonstrated that J774.1 macrophages expressed considerable amount of mRNA and reductase activity of 11β-HSD1. Our data is the first to demonstrate that the cell activation with LPS markedly augmented mRNA expression and reductase activity of 11β-HSD1, accompanied by a drastic morphological change and increased secretion of pro-inflam-

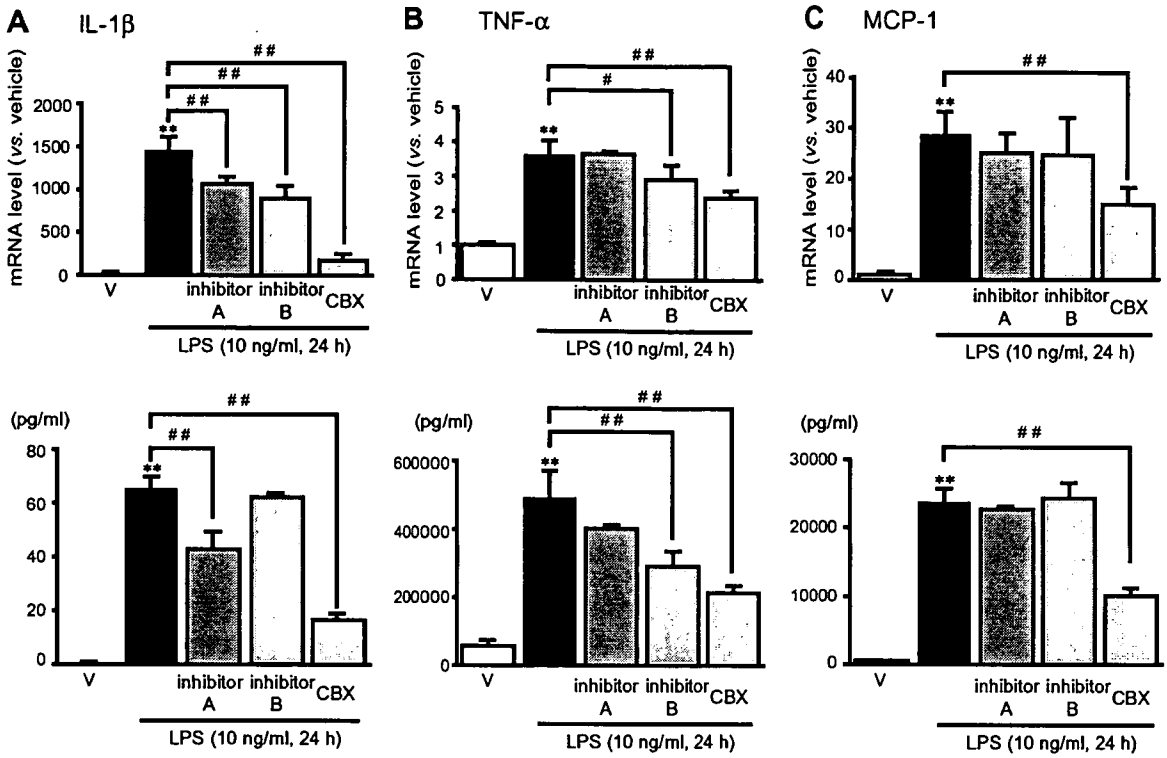

Fig. 3. Pharmacological inhibition of 11β-HSD1 considerably reduced IL-1 β, TNF-α or MCP-1 expression in and secretion from LPS-activated J774.1 macrophages. Effect of pharmacological inhibition of 11β-HSD1 on (A) IL-1β, (B) TNF-α and (C) MCP-1 mRNA in and secretion from LPS-activated J774.1 macrophages: J774.1 cells were activated by LPS (10 ng/ml) and co-treated with inhibitor A (10 μM), inhibitor B (100 μM) or CBX (100 μM) for 24 h. (upper); mRNA for IL-1β, TNF-α and MCP-1 determined by real-time PCR. Level of each mRNA was normalized to that of 18S rRNA and expressed as a relative value vs. control (lower). Concentrations of IL-1β, TNF-α and MCP-1 in the media measured by ELISA. Data are expressed as means ± S.E.M. of triplicate experiments. $^{**}P < 0.01$ vs. vehicle (V) treated group. $^{\#}P < 0.05$, $^{\#\#}P < 0.01$ vs. LPS-treated cells.

matory cytokines [13]. Recent studies highlighted the concept that not only LPS but non-microbial molecules such as fatty acids can also activate macrophages through TLR4 [21]. It is also suggested that endogenous, intestine-derived LPS contributes to the pathophysiology of obesity-associated fatty liver diseases [22]. In this context, potential mechanism of LPS-mediated dysfunction of adipose tissue stimulates much interest in future studies.

Glucocorticoids are widely used as anti-inflammatory agents in human clinics [23]. Consistent with the notion that glucocorticoids act as anti-inflammatory hormones, our data demonstrated that treatment of J774.1 cells with dexamethasone significantly suppressed the mRNA expression and secretion of IL-1β, TNF-α and MCP-1 in a dose-dependent manner (supplementary figure). On the other hand, physiological effects of endogenous glucocorticoids are distinct from those in pharmacological or therapeutic concentrations of synthetic cortisol analogues [24–27]. A recent study showed that 11β-HSD1-mediated intracellular glucocorticoid reamplification in macrophages enhanced phagocytic activity [28]. However, it still remains controversial whether the activation of 11β-HSD1 is involved in pro-inflammatory properties of macrophages. To test the possibility, we assessed the potential impact of pharmacological inhibition of 11β-HSD1 on secretion of pro-inflammatory cytokine and chemokine. Our data demonstrated for the first time that treatment of J774.1 cells with three structurally distinct 11β-HSD1 inhibitors considerably suppressed the mRNA expression and secretion of IL-1β, TNF-α or MCP-1, clearly indicating that intracellular regeneration of active glucocorticoid via 11β-HSD1 does exert pro-inflammatory effects on activated macrophages. Taking structural and pharmacological differences of compounds into consideration, further investigation is required to reinforce the result.

Macrophages play pathophysiologic roles in adipose dysfunction, arteriosclerosis [16] and inflammatory fatty liver diseases [22]. A recent study showed that pharmacologic inhibition of 11β-HSD1 ameliorated diabetes, dyslipidemia [29] and arteriosclerosis [16] in mouse models. It should also be noted that, reminiscent of adipocytes [16]. 11β-HSD1 expression and reductase activity is predominated in macrophages (Fig. 1), while that of 11β-HSD2 and dehydrogenase activity were not detected in our assays (data not shown). Taken together, our results suggest that 11β-HSD1 in activated macrophages may be a novel target for the treatment of metabolic diseases.

In adipose tissue, 11β-HSD1 was expressed not only in mature adipocytes but also stromal vascular fraction (SVF) cells which include infiltrated macrophages [30]. Number of cells contained in SVF was estimated to be two-thirds of that in whole adipose tissue [31]. Our data in human adipose tissue biopsies also showed that SVF from adipose tissue expressed 11β-HSD1 to a considerable extent (approximately 20% of that in floating matured adipocytes) (Yasue, S. et al. manuscript in preparation). Thus, 11β-HSD1 in activated macrophages may play a role in the pathophysiology of adipose

inflammation and dysfunction. Further investigations in vivo should validate this notion and may open a fresh avenue for molecular and cellular mechanism of adipose inflammation and dysfunction.

Acknowledgements: We thank Dr. Y. Tominaga and S. Yokota (Kaneka Co. Osaka, Japan) for valuable help in the microsome assay, Dr. M. Fujimoto for critical discussion, and Ms. S. Masumoto, K. Takahashi, S. Maki and M. Nagamoto for assistance. This work was supported in part by Grant-in-Aid for Scientific Research (B2; 16390267), (S2; 16109007), Grant-in-Aid for Scientific Research on Priority Areas (adipomics, 15081101), Grant-in-Aid for Research on Measures for Intractable Diseases (Health and Labor Science Research Grant), Research Grant from Special Coordination Funds for Promoting Science and Technology (JST), AstraZeneca International Research Grant, Takeda Medical Research Foundation, Smoking Research Foundation, Metabolic Syndrome Foundation and Setsuro Fujii Memorial Osaka Foundation for Promotion of Fundamental Medical Research.

Appendix A. Supplementary data

Supplementary data associated with this article can be found, in the online version, at doi:10.1016/j.febslet.2006.11.032.

References

[1] Ford, E.S., Giles, W.H. and Dietz, W.H. (2002) Prevalence of the metabolic syndrome among US adults: findings from the third National Health and Nutrition Examination Survey. Jama 287, 356–359.
[2] Bujalska, I.J., Kumar, S. and Stewart, P.M. (1997) Does central obesity reflect "Cushing's disease of the omentum? Lancet 349, 1210–1213.
[3] Jamieson, P.M., Chapman, K.E., Edwards, C.R. and Seckl, J.R. (1995) 11β-hydroxysteroid dehydrogenase is an exclusive 11 beta-reductase in primary cultures of rat hepatocytes: effect of physicochemical and hormonal manipulations. Endocrinology 136, 4754–4761.
[4] Wake, D.J. and Walker, B.R. (2004) 11 beta-hydroxysteroid dehydrogenase type 1 in obesity and the metabolic syndrome. Mol. Cell Endocrinol. 215, 45–54.
[5] Masuzaki, H., Paterson, J., Shinyama, H., Morton, N.M., Mullins, J.J., Seckl, J.R. and Flier, J.S. (2001) A transgenic model of visceral obesity and the metabolic syndrome. Science 294, 2166–2170.
[6] Masuzaki, H. et al. (2003) Transgenic amplification of glucocorticoid action in adipose tissue causes high blood pressure in mice. J. Clin. Invest. 112, 83–90.
[7] Morton, N.M. et al. (2004) Novel adipose tissue-mediated resistance to diet-induced visceral obesity in 11 beta-hydroxysteroid dehydrogenase type 1-deficient mice. Diabetes 53, 931–938.
[8] Kotelevtsev, Y. et al. (1997) 11beta-hydroxysteroid dehydrogenase type 1 knockout mice show attenuated glucocorticoid-inducible responses and resist hyperglycemia on obesity or stress. Proc. Natl. Acad. Sci. USA 94, 14924–14929.
[9] Harris, H.J., Kotelevtsev, Y., Mullins, J.J., Seckl, J.R. and Holmes, M.C. (2001) Intracellular regeneration of glucocorticoids by 11beta-hydroxysteroid dehydrogenase (11beta-HSD)-1 plays a key role in regulation of the hypothalamic-pituitary-adrenal axis: analysis of 11beta-HSD-1-deficient mice. Endocrinology 142, 114–120.
[10] Weisberg, S.P., McCann, D., Desai, M., Rosenbaum, M., Leibel, R.L. and Ferrante Jr., A.W. (2003) Obesity is associated with macrophage accumulation in adipose tissue. J. Clin. Invest. 112, 1796–1808.
[11] Xu, H. et al. (2003) Chronic inflammation in fat plays a crucial role in the development of obesity-related insulin resistance. J. Clin. Invest. 112, 1821–1830.
[12] Suganami, T., Nishida, J. and Ogawa, Y. (2005) A paracrine loop between adipocytes and macrophages aggravates inflammatory changes: role of free fatty acids and tumor necrosis factor alpha. Arterioscler. Thromb. Vasc. Biol. 25, 2062–2068.
[13] Ralph, P. and Nakoinz, I. (1975) Phagocytosis and cytolysis by a macrophage tumour and its cloned cell line. Nature 257, 393–394.
[14] Andrews, R.C., Rooyackers, O. and Walker, B.R. (2003) Effects of the 11 beta-hydroxysteroid dehydrogenase inhibitor carbenoxolone on insulin sensitivity in men with type 2 diabetes. J. Clin. Endocrinol. Metab. 88, 285–291.
[15] Sandeep, T.C., Andrew, R., Homer, N.Z., Andrews, R.C., Smith, K. and Walker, B.R. (2005) Increased in vivo regeneration of cortisol in adipose tissue in human obesity and effects of the 11beta-hydroxysteroid dehydrogenase type 1 inhibitor carbenoxolone. Diabetes 54, 872–879.
[16] Hermanowski-Vosatka, A. et al. (2005) 11beta-HSD1 inhibition ameliorates metabolic syndrome and prevents progression of atherosclerosis in mice. J. Exp. Med. 202, 517–527.
[17] Hult, M. et al. (2006) Active site variability of type 1 11beta-hydroxysteroid dehydrogenase revealed by selective inhibitors and cross-species comparisons. Mol. Cell Endocrinol. 248, 26–33.
[18] Wang, S.J. et al. (2006) Inhibition of 11beta-hydroxysteroid dehydrogenase type 1 reduces food intake and weight gain but maintains energy expenditure in diet-induced obese mice. Diabetologia 49, 1333–1337.
[19] Poltorak, A. et al. (1998) Defective LPS signaling in C3H/HeJ and C57BL/10ScCr mice: mutations in Tlr4 gene. Science 282, 2085–2088.
[20] Hoshino, K., Takeuchi, O., Kawai, T., Sanjo, H., Ogawa, T., Takeda, Y., Takeda, K. and Akira, S. (1999) Cutting edge: toll-like receptor 4 (TLR4)-deficient mice are hyporesponsive to lipopolysaccharide: evidence for TLR4 as the Lps gene product. J. Immunol. 162, 3749–3752.
[21] Lee, J.Y., Sohn, K.H., Rhee, S.H. and Hwang, D. (2001) Saturated fatty acids, but not unsaturated fatty acids, induce the expression of cyclooxygenase-2 mediated through Toll-like receptor 4. J. Biol. Chem. 276, 16683–16689.
[22] Yang, S.Q., Lin, H.Z., Lane, M.D., Clemens, M. and Diehl, A.M. (1997) Obesity increases sensitivity to endotoxin liver injury: implications for the pathogenesis of steatohepatitis. Proc. Natl. Acad. Sci. USA 94, 2557–2562.
[23] Rhen, T. and Cidlowski, J.A. (2005) Antiinflammatory action of glucocorticoids – new mechanisms for old drugs. N. Engl. J. Med. 353, 1711–1723.
[24] Barber, A.E., Coyle, S.M., Marano, M.A., Fischer, E., Calvano, S.E., Fong, Y., Moldawer, L.L. and Lowry, S.F. (1993) Glucocorticoid therapy alters hormonal and cytokine responses to endotoxin in man. J. Immunol. 150, 1999–2006.
[25] Liao, J., Keiser, J.A., Scales, W.E., Kunkel, S.L. and Kluger, M.J. (1995) Role of corticosterone in TNF and IL-6 production in isolated perfused rat liver. Am. J. Physiol. 268, R699–R706.
[26] Sapolsky, R.M., Romero, L.M. and Munck, A.U. (2000) How do glucocorticoids influence stress responses? Integrating permissive, suppressive, stimulatory, and preparative actions. Endocr. Rev. 21, 55–89.
[27] Smyth, G.P., Stapleton, P.P., Freeman, T.A., Concannon, E.M., Mestre, J.R., Duff, M., Maddali, S. and Daly, J.M. (2004) Glucocorticoid pretreatment induces cytokine overexpression and nuclear factor-kappaB activation in macrophages. J. Surg. Res. 116, 253–261.
[28] Gilmour, J.S. et al. (2006) Local amplification of glucocorticoids by 11beta-hydroxysteroid dehydrogenase type 1 promotes macrophage phagocytosis of apoptotic leukocytes. J. Immunol. 176, 7605–7611.
[29] Alberts, P. et al. (2003) Selective inhibition of 11 beta-hydroxysteroid dehydrogenase type 1 improves hepatic insulin sensitivity in hyperglycemic mice strains. Endocrinology 144, 4755–4762.
[30] Paulmyer-Lacroix, O., Boullu, S., Oliver, C., Alessi, M.C. and Grino, M. (2002) Expression of the mRNA coding for 11beta-hydroxysteroid dehydrogenase type 1 in adipose tissue from obese patients: an in situ hybridization study. J. Clin. Endocrinol. Metab. 87, 2701–2705.
[31] Rodbell, M. (1964) Localization of lipoprotein lipase in fat cells of rat adipose tissue. J. Biol. Chem. 239, 753–755.

0021-972X/07/$15.00/0
Printed in U.S.A.

The Journal of Clinical Endocrinology & Metabolism 92(2):532–541

doi: 10.1210/jc.2006-1546

Efficacy and Safety of Leptin-Replacement Therapy and Possible Mechanisms of Leptin Actions in Patients with Generalized Lipodystrophy

Ken Ebihara, Toru Kusakabe, Masakazu Hirata, Hiroaki Masuzaki, Fumiko Miyanaga, Nozomi Kobayashi, Tomohiro Tanaka, Hideki Chusho, Takashi Miyazawa, Tatsuya Hayashi, Kiminori Hosoda, Yoshihiro Ogawa, Alex M. DePaoli, Masanori Fukushima, and Kazuwa Nakao

Department of Medicine and Clinical Science (K.E., T.K., M.H., H.M., F.M., N.K., T.T., H.C., T.M., T.H., K.H., Y.O., K.N.), Kyoto University Graduate School of Medicine, and Department of Clinical Trial Management (M.F.), Translational Research Center, Kyoto University Hospital, Kyoto 606-8507, Japan; and Amgen Inc. (A.M.D.), Thousand Oaks, California 91319

Background: Lack of leptin is implicated in insulin resistance and other metabolic abnormalities in generalized lipodystrophy; however, the efficacy, safety, and underlying mechanisms of leptin-replacement therapy in patients with generalized lipodystrophy remain unclear.

Methods: Seven Japanese patients with generalized lipodystrophy, two acquired and five congenital type, were treated with the physiological replacement dose of recombinant leptin during an initial 4-month hospitalization followed by outpatient follow-up for up to 36 months.

Results: The leptin-replacement therapy with the twice-daily injection dramatically improved fasting glucose (mean ± SE, 172 ± 20 to 120 ± 12 mg/dl, $P < 0.05$) and triglyceride levels (mean ± SE, 700 ± 272 to 260 ± 98 mg/dl, $P < 0.05$) within 1 wk. The leptin-replacement therapy reduced insulin resistance evaluated by euglycemic clamp method and augmented insulin secretion at glucose tolerance test with different responses between acquired and congenital types. Improvement of the fatty liver was also observed. The efficacy and safety of the once-daily injection were comparable to those of the twice-daily injection. The leptin-replacement therapy ameliorated macro- and microalbuminuria and showed no deterioration of neuropathy and retinopathy of these patients. The leptin-replacement therapy is beneficial to diabetic complications and lipodystrophic ones. Two patients developed antileptin antibodies but not neutralizing antibodies. The therapy was well tolerated, and its effects were maintained for up to 36 months without any notable adverse effects such as hypoglycemia, high blood pressure, or reduction of bone mineral density.

Conclusions: The present study demonstrates the efficacy and safety of the long-term leptin-replacement therapy and possible mechanisms of leptin actions in patients with generalized lipodystrophy. (*J Clin Endocrinol Metab* **92: 532–541, 2007**)

LEPTIN PLAYS A MAJOR role in the regulation of energy homeostasis (1). The plasma leptin concentration increases in proportion to the degree of adiposity (2–6). Besides the antiobesity actions, leptin has a wide range of actions including antidiabetic actions (6–8).

Generalized lipodystrophy is a heterogeneous group of diseases characterized by a profound deficiency of adipose tissue (9) and is commonly associated with severe insulin-resistant diabetes, hypertriglyceridemia, and fatty liver (10, 11). In lipoatrophic patients, these metabolic abnormalities develop as a consequence of decreased mass of the adipose tissue (12–14), and consequently, plasma leptin concentrations are markedly reduced (15). We and others demonstrated that the leptin administration or transgenic overexpression of leptin reverses the metabolic abnormalities in different mouse models of lipodystrophy, indicating that the metabolic abnormalities in lipoatrophic patients are caused mainly by a shortage of leptin (16, 17). Recently, the 4-month leptin-replacement therapy with twice-daily injection protocol was reported to improve glucose and lipid metabolism in nine female patients with lipodystrophy in the United States (18).

In the present study, we evaluated the efficacy and safety of long-term leptin-replacement therapy on seven Japanese patients with generalized lipodystrophy.

First Published Online November 21, 2006

Abbreviations: AGL, Acquired generalized lipodystrophy; CGL, congenital generalized lipodystrophy; CT, computed tomography; HbA1c, glycosylated hemoglobin; L/S, liver to spleen; r-metHuLeptin, recombinant methionyl human leptin.

Subjects and Methods

Subjects

Eligible criteria were according to the study protocol of the National Institutes of Health (18). We evaluated seven patients with generalized lipodystrophy including two patients with acquired generalized lipodystrophy (AGL) and five patients with congenital generalized lipodystrophy (CGL). Patients with CGL were further analyzed for mutations in either *seipin* (19) or 1-acylglycerol-3-phosphate *O*-acyltransferase2 (*AGPAT2*) genes (20). Table 1 summarizes the baseline clinical characteristics of seven patients treated in the present study.

Study design

The study protocol was approved by the ethical committee of Kyoto University Graduate School of Medicine (approval number 331). Informed written consent was obtained from all subjects and their families. Recombinant methionyl human leptin (r-metHuLeptin) was provided by Amgen, Inc. (Thousand Oaks, CA). For the first year, r-metHuLeptin